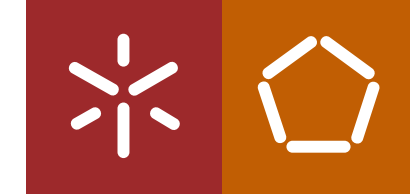


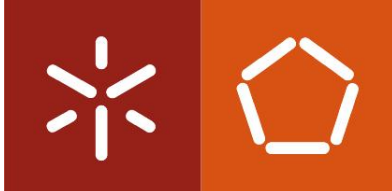


Marisa da Conceição Gomes Lopes

**Optimization of *Candida albicans* Biofilms
Inactivation by Benzophenoxazine Compounds
for Photodynamic Therapy**

Universidade do Minho
Escola de Engenharia





Universidade do Minho

Escola de Engenharia

Marisa da Conceição Gomes Lopes

**Optimization of *Candida albicans* Biofilms
Inactivation by Benzophenoxazine Compounds
for Photodynamic Therapy**

Dissertação de Mestrado

Mestrado Integrado em Engenharia Biomédica

Trabalho efetuado sob a orientação da

Professora Doutora Isabel Maria Pires Belo

**Professora Doutora Mariana Contente Rangel
Henriques**

Outubro de 2013

DECLARAÇÃO

Nome: Marisa da Conceição Gomes Lopes

Endereço eletrónico: a55582@alunos.uminho.pt

Telefone: 91 285 63 07

Número do Bilhete de Identidade: 13790943

Título dissertação/tese: Optimization of *Candida albicans* biofilms inactivation by benzophenoxazine compounds for photodynamic therapy

Ano de conclusão: 2013

Orientador(es): Professora Doutora Isabel Maria Pires Belo

Professora Doutora Mariana Contente Rangel Henriques

Designação do Mestrado: Mestrado Integrado em Engenharia Biomédica

Área de Especialização: Engenharia Clínica

Escola: de Engenharia

Departamento: de Engenharia Biológica

DE ACORDO COM A LEGISLAÇÃO EM VIGOR, NÃO É PERMITIDA A REPRODUÇÃO DE QUALQUER PARTE DESTA TESE/TRABALHO

Universidade do Minho, ____ / ____ / ____

Assinatura: _____

ACKNOWLEDGEMENTS

First of all, I want to express my gratitude to my supervisors Dr. Isabel Belo and Dr. Mariana Henriques. This work would not have been possible without them. To Dr. Isabel Belo I want especially to thank the availability of guidance, the knowledge, sympathy and the encouragement which were essential to my self-confidence, autonomy and organization. To Dr. Mariana Henriques, I want especially express my gratefulness for the knowledge, dedication and time spent put on my dissertation. All the advices, suggestions and encouragement that she gave me during the experimental work and dissertation-writing period were very important.

I have to express my gratefulness to Dr. Maria Sameiro Gonçalves for her availability and for gently provide the benzophenoxazine compounds, as well as to thank to Dr. Paulo Coutinho for the permission to use the irradiation systems, for all the support, knowledge and suggestions.

To Carlos Tiago Alves I want to express my gratefulness for all the time he spent with me and the support in the lab, as well as all the teaching, the encouragement, the friendship and the advices he devoted to me during all stages of this work. I have no words to express how his support was important to me.

To Dr. Sónia Silva I want to thank for all the teaching, support, availability, patience and hospitality in the lab which were essential for me to learn and develop my experimental work. Additionally, I have to recognize all the members of the lab for the hospitality and the sharing of experiences. They made me feel a part of the group.

I am also grateful to my closest friends and course colleagues for the friendship, affection, sharing of experiences and good moments during all these years. I learned and grew very much at their side and I am glad for being with them during this long walk.

To Elson Pina I want to thank all the affection, love, encouragement and patience that has always held for me, particularly in the most difficult days. He was my safe haven and his emotional support was very important to keep me motivated during the development of this work.

Finally, the last words are addressed to my beloved family, my parents and my sister. I am deeply grateful to them for all the education, values, love, affection, as well as their emotional support and continuous encouragement to get through difficult times and to achieve my goals.

ABSTRACT

The incidence of fungal infections has increased in the last decades, being *Candida albicans* the most common etiologic agent of fungal-related biofilm infections. In the last years, *Candida* strains have shown high levels of drug resistance, so the interest in new antifungal therapeutic options has increased. The antimicrobial photodynamic therapy (APDT) has been shown to be an emerging and promising approach to treat localized infections. The present dissertation aimed to optimize the antifungal photodynamic efficacy of two new benzophenoxazine-type fluorescent dyes against *C. albicans* biofilms by APDT, as well as to understand the different APDT outcomes achieved.

The antifungal susceptibility of *C. albicans* planktonic cells to dyes *N*[5-(3-hydroxypropylamino)-10-methyl-9*H*benzo[*a*]phenoxazin-9-ylidene]ethanaminium chloride (FSc) and *N*(5-(11-hydroxyundecylamino)-10-methyl-9*H*benzo[*a*]phenoxazin-9-ylidene)ethanaminium chloride (FSd) with concentrations in the range of 0-100 μ M during 48 h was firstly determined. The potential photodynamic activity of dyes against *C. albicans* biofilms was then evaluated and optimized by incubation of biofilms with dyes in the range of 100-300 μ M for 3 or 18 h followed by illumination at fluences of 12 or 36 J cm⁻² through the use of a xenon arc lamp (600 \pm 2 nm). In order to understand the APDT outcomes achieved, dye uptake by the biofilm matrix and cells during dark incubation was also evaluated by spectrofluorimetric analysis (λ_{ex} =590 nm; λ_{em} =645 nm) and fluorescence microscopy.

On antifungal susceptibility assays, FSc dye showed no growth inhibition of *C. albicans* cells, while FSd produced a very poor growth inhibition when used at 50 and 100 μ M. Regarding to APDT outcomes, only FSc dye showed to have photosensitizing activity against *C. albicans* biofilms. Using FSc at 300 μ M for 18 h followed by illumination with 36 J cm⁻² of fluence, a total photoinactivation of *C. albicans* biofilm cells was achieved. The notorious uptake of FSc over FSd dye by biofilms may explain its higher photodynamic effectiveness.

In summary, data suggests that FSc-mediated APDT might be successfully used to treat *C. albicans* infections.

RESUMO

A incidência de infecções fúngicas tem aumentado nas últimas décadas, sendo a espécie *C. albicans* o agente etiológico mais comum nas infecções causadas por biofilmes. Nos últimos anos, as estirpes do género *Candida* têm demonstrado elevados níveis de resistência aos agentes antifúngicos convencionais, impulsionando o interesse por novas terapias antifúngicas. A fototerapia dinâmica antimicrobiana é uma nova abordagem terapêutica que se tem demonstrado bastante promissora no tratamento de infecções localizadas. A presente dissertação teve como objetivo otimizar a inativação de biofilmes de *C. albicans* pela ação fotodinâmica antifúngica de dois novos corantes fluorescentes do tipo benzofenoxazina, assim como analisar as diferentes eficácias fotodinâmicas encontradas.

Inicialmente determinou-se a suscetibilidade antifúngica aos corantes cloreto de *N*-(5-((3-hidroxipropil)amino)-10-metil-9*H*-benzo[*a*]fenoxazina-9-ilidene)etanamínio (FSc) e cloreto de *N*-(5-((11-hidroxoundecil)amino)-10-metil-9*H*-benzo[*a*]fenoxazina-9-ilidene)etanamínio (FSd) - utilizando concentrações de 0-100 μM durante 48 h em células planctónicas de *C. albicans*. A potencial atividade fotodinâmica dos corantes em biofilmes de *C. albicans* foi posteriormente avaliada e otimizada incubando os biofilmes de *C. albicans* com os corantes com concentrações de 100-300 μM durante 3 ou 18 h, seguido de irradiação com uma lâmpada de arco de xénon (600 ± 2 nm) com fluência de 12 ou 36 J cm^{-2} . Com o intuito de entender as diferentes eficácias fotodinâmicas observadas, foi também avaliada a absorção dos corantes por espectrofluorimetria ($\lambda_{\text{ex}}=590$ nm; $\lambda_{\text{em}}=645$ nm) e microscopia de fluorescência.

Os ensaios de suscetibilidade antifúngica revelaram que o corante FSc não apresenta efeito de inibição de crescimento, enquanto o corante FSd produz um pequeno efeito de inibição do crescimento quando utilizado a 50 ou 100 μM . Relativamente à ação fotodinâmica antimicrobiana apenas o corante FSc demonstrou ter atividade fotossensibilizante nos biofilmes de *C. albicans*. Da incubação dos biofilmes com corante FSc a 300 μM durante 18 h, seguido de irradiação com 36 J cm^{-2} de fluência, obteve-se uma total inativação celular. A notória absorção do corante FSc em relação ao FSd pelos biofilmes poderá explicar a sua maior eficácia fotodinâmica. Em suma, os resultados indicam que o corante FSc poderá ser um potencial agente fotossensibilizante para a fototerapia dinâmica antifúngica de infecções provocadas por *C. albicans*.

TABLE OF CONTENTS

AKNOWLEDGEMENTS	iii
ABSTRACT	v
RESUMO	vii
TABLE OF CONTENTS	ix
LIST OF FIGURES	xiii
LIST OF TABLES	xvii
ABBREVIATIONS.....	xix
SYMBOLS.....	xxi
PREAMBLE.....	xxiii
1. CHAPTER I - INTRODUCTION.....	1
1.1. <i>Candida albicans</i>	3
1.1.1. The Role of <i>C. albicans</i> Cell Wall	4
1.1.2. Virulence Factors of <i>C. albicans</i>	4
1.1.3. The Role of Biofilm in Antifungal Agents Resistance	8
1.2. ANTIMICROBIAL PHOTODYNAMIC THERAPY (APDT)	11
1.2.1. Photophysical processes of PDT	12
1.2.2. The Photobleaching Process	14
1.2.3. Mechanism of Action of APDT	14
1.2.4. Biofilms eradication by APDT	16
1.2.5. Cellular Resistance Mechanisms to APDT	17
1.2.6. Applications of APDT	18
1.3. PHOTSENSITIZERS	19
1.3.1. Properties of Photosensitizers	19
1.3.2. Most Common Photosensitizers in APDT	22
1.3.3. Benzo[a]phenoxazines	24

1.3.4. Formulation of New Concepts	26
1.4. LIGHT SOURCES AND DELIVERY	26
1.4.1. The concept of Light Fluence and Source Irradiance	26
1.4.2. Light Penetration	27
1.4.3. Most Common Light Sources in PDT	27
2.CHAPTER II - MATERIALS AND METHODS	29
2.1. Benzophenoxazines Origin	31
2.2. Benzophenoxazines Stock Solutions	31
2.3. Organism, Culture Media and Growth Conditions.....	32
2.4. Antifungal Susceptibility Testing	33
2.5. Biofilm Formation	33
2.6. Quantification of Cultivable Biofilm Cells.....	33
2.7. Antifungal Photodynamic Therapy	34
2.7.1. Dark Toxicity	34
2.7.2 Photodynamic Inactivation	34
2.7.3. Absorption Spectra of Biofilms	35
2.8. Dye Uptake.....	35
2.9. Fluorescence Microscopy.....	36
2.9.1. Fluorescence Microscopy of Planktonic Cells.....	36
2.9.2. Fluorescence Microscopy of Biofilm Resuspended Cells.....	37
2.10. Statistical Analysis	37
3. CHAPTER III - RESULTS AND DISCUSSION	39
3.1. Antifungal Susceptibility Testing	41
3.2. Antifungal Photodynamic Therapy	42
3.3. Dye Uptake.....	47

4. CHAPTER IV - CONCLUSIONS AND FUTURE PERSPECTIVES.....	54
5. REFERENCES.....	59
6. APPENDICES.....	71
Appendix A - Absorption Spectra of Biofilms.....	73
Appendix B - Calibration Curves	77

LIST OF FIGURES

CHAPTER I - INTRODUCTION

Figure 1. Illustration of steps in <i>Candida albicans</i> biofilm formation. 1 and 2. Formation begins with adhesion of yeast cells to a surface by nonspecific interactions, such as hydrophobic and electrostatic forces, as well as specific adhesin-ligand bonds. 3. Attached cells proliferate to form microcolonies and start to deposit the ECM. 4. The biofilm grows into a thick layer where ECM involves a complex network of yeast cells, hyphae and pseudohyphae. 5. Cells released or detached from the biofilm spread into the environment, dispersing infections and forming new biofilms.	7
Figure 2. Schematic illustration of photodynamic therapy mechanism of action.....	12
Figure 3. Illustrative scheme of essential steps involved on antifungal photodynamic therapy... .	15
Figure 4. Chemical structures of the main photosensitizers used on PDT.....	22
Figure 5. (A) Chemical structure of phenoxazines and benzophenoxazines; (B) Structures of the three best known benzo[<i>a</i>]phenoxazines..	25

CHAPTER II - MATERIALS AND METHODS

Figure 6. Chemical structure of FSc (A) and FSd (B) dyes.....	31
---	----

CHAPTER III - RESULTS AND DISCUSSION

Figure 7. Susceptibility of <i>C. albicans</i> ATCC 90028 planktonic cells exposed for 48 h to FSc (A) and FSd (B) dye in RPMI. Error bars represent standard deviation. *Statistically different from the respective control, 0 μ M ($P < 0.05$).....	41
Figure 8. Logarithm of number of <i>C. albicans</i> ATCC 90028 biofilm cells per cm ² after 3 h of dark incubation with FSc (A) and FSd (B) dye at different concentrations in PBS. Error bars represent standard deviation. *Statistically different from the control, 0 μ M ($P < 0.05$).	43
Figure 9. Logarithm of number of <i>C. albicans</i> ATCC 90028 biofilm cells per cm ² after 3 h of dark incubation with FSc (A) and FSd (B) dye at different concentrations in PBS followed of exposure to various light doses. Error bars represent standard deviation. *Statistically different from the control, 0 μ M ($P < 0.05$).....	44

Figure 10. Logarithm of number of <i>C. albicans</i> ATCC 90028 biofilm cells per cm ² after 18 h of dark incubation with both FSc and FSd dyes at different concentrations in PBS. Error bars represent standard deviation. * Statistically different from the control, 0 µM ($P<0.05$).	44
Figure 11. Logarithm of number of <i>C. albicans</i> ATCC 90028 biofilm cells per cm ² after 18 h of dark incubation with FSc (A) and FSd (B) dye at different concentrations in PBS followed of exposure to various light doses. Error bars represent standard deviation.*Statistically different from the control, 0 µM ($P<0.05$).	45
Figure 12. Fluorescence microscopy micrographs obtained for <i>C. albicans</i> ATCC 90028 planktonic cells after 3 h of incubation (A1-A3) and 18 h of incubation (B1-B3) with PBS only, as well as with FSc and FSd dye at 300 µM in PBS.	50
Figure 13. Fluorescence microscopy micrographs obtained for <i>C. albicans</i> ATCC 90028 biofilm resuspended cells after 3 h of dark incubation (A1-A3) and 18 h of dark incubation (B1-B3) with PBS only, as well as with FSc and FSd dye at 300 µM in PBS.	51

APPENDICES – APPENDIX A

Figure A 1. Absorption spectra of biofilms of <i>Candida albicans</i> ATCC 90028 before and after exposure to a light fluence of 12 J cm ⁻² following 3 h of incubation with FSc dye at 100 µM (A), 200 µM (B) and 300 µM (C) in PBS.	73
Figure A 2. Absorption spectra of biofilms of <i>Candida albicans</i> ATCC 90028 before and after exposure to a light fluence of 12 J cm ⁻² following 3 h of incubation with FSd dye at a 100 µM (A), 200 µM (B) and 300 µM (C) in PBS.	73
Figure A 3. Absorption spectra of biofilms of <i>Candida albicans</i> ATCC 90028 before and after exposure to a light fluence of 36 J cm ⁻² following 3 h of incubation with FSc dye at 100 µM (A), 200 µM (B) and 300 µM (C) in PBS.	74
Figure A 4. Absorption spectra of biofilms of <i>Candida albicans</i> ATCC 90028 before and after exposure to a light fluence of 36 J cm ⁻² following 3 h of incubation with FSd dye at 100 µM (A), 200 µM (B) and 300 µM (C) in PBS.	74
Figure A 5. Absorption spectra of biofilms of <i>Candida albicans</i> ATCC 90028 before and after exposure to a light fluence of 12 J cm ⁻² following 18 h of incubation with FSc dye at 100 µM (A), 200 µM (B) and 300 µM (C) in PBS.	75

Figure A 6. Absorption spectra of biofilms of <i>Candida albicans</i> ATCC 90028 before and after exposure to a light fluence of 36 J cm^{-2} following 18 h of incubation with FSc dye at 100 μM (A), 200 μM (B) and 300 μM (C) in PBS.	75
Figure A 7. Absorption spectra of biofilms of <i>Candida albicans</i> ATCC 90028 before and after exposure to a light fluence of 36 J cm^{-2} following 18 h of incubation with FSd dye at 100 μM (A), 200 μM (B) and 300 μM (C) in PBS.	76

APPENDICES – APPENDIX B

Figure B 1. Calibration curve of absorbance versus FSc dye concentration.....	77
Figure B 2. Calibration curve of absorbance versus FSd dye concentration.....	77
Figure B 3. Calibration curve of fluorescence intensity versus FSc dye concentration.....	78
Figure B 4. Calibration curve of fluorescence intensity versus FSd dye concentration.	78

LIST OF TABLES

CHAPTER I - INTRODUCTION

Table 1. Profile of an ideal photosensitizer for APDT use in the clinical field.	21
Table 2. Lamps and lasers more frequent used on PDT applications.....	28

CHAPTER II - MATERIALS AND METHODS

Table 3. Photophysical properties of pertinent dyes.	31
---	----

CHAPTER III - RESULTS AND DISCUSSION

Table 4. Uptake of FSc and FSd by biofilms of <i>C. albicans</i> ATCC 90028 after dark incubation with both dyes at 100 and 300 μ M in PBS for 3 h or 18 h. The values are means \pm Standard deviations.....	48
---	----

ABBREVIATIONS

ABC	ATP-binding Cassette
Abs	Absorbance
ALA	5-Aminolevulinic acid
Als	Agglutinin-like sequence
ANOVA	Analysis of Variance
APDT	Antimicrobial Photodynamic Therapy
ATCC	American Type Culture Collection
ATP	Adenosine Triphosphate
cAMP	Cyclic Adenosine Monophosphate
CDR	Complementarity-determining regions
CFU	Colony forming units
CLSI	Clinical and Laboratory Standards Institute
DNA	Deoxyribonucleic acid
FDA	Food and Drug Administration
HIV	Human Immunodeficiency Virus
HP	Hematoporphyrin
HPD	Hematoporphyrin Derivative
HSP	Heat Shock Proteins
MAPK	Mitogen-activated Protein Kinase
MB	Methylene Blue
MDR	Multidrug Resistance
MFS	Major Facilitator Superfamily
MOPS	3-(N-Morpholino)propanesulfonic acid, 4-Morpholinepropanesulfonic acid
NCCLS	National Committee for Clinical Laboratory Standards

PBS	Phosphate Buffered Saline
PKA	Protein Kinase A
Pp	Protoporphyrin
RNA	Ribonucleic acid
rpm	Revolutions per minute
Ras	Rat Sarcoma
RPMI	Roswell Park Memorial Institute
SAP	Stress Associated Protein
Saps	Secreted Aspartyl Proteinases
SDA	Sabouraud Dextrose Agar
SDB	Sabouraud Dextrose Broth
TBO	Toluidine Blue
TRITC	Tetramethylrhodamine Isothiocyanate

SYMBOLS

λ_{max}	Wavelength of maximum absorption
ε	Extinction coefficient
τ_t	Triplet-state life time
Φ_t	Triplet-state quantum yield
ΔE_t	Triplet-state energy
Φ_Δ	Singlet oxygen quantum yield
λ_{ex}	Excitation wavelength
λ_{em}	Emission wavelength
Φ_F	Absolute fluorescence quantum yield
g	Gravity constant
P	Significance value

PREAMBLE

In the last decades, the incidence of superficial and systemic fungal infections has increased due to several factors, including the more frequent use of invasive procedures, prosthetic devices, immunosuppressive medication and broad-spectrum antibiotics, as well as the increased incidence of neutropenia and HIV infections [1]. Yeasts from the genus *Candida* are responsible for 70-90% of the fungal infections cases, with *Candida albicans* representing about 50% of all yeasts isolated in clinical samples [2, 3]. In fact, *C. albicans* is the most virulent *Candida* species and represents an important public health challenge with a high economic and medical relevance due to the increased costs of care, time of hospitalization and high morbidity and mortality rates, especially on immunocompromised patients [4]. In this context, conventional approaches of antifungal therapies can be time consuming, expensive and in the last years they have been largely associated with the emergence of resistant strains [5]. Thus, nowadays there is an increased necessity to discover alternative, more effective and localized antifungal therapeutic options to treat fungal infections [3].

The photodynamic therapy (PDT), originally developed for the treatment of skin tumors, has been shown as an effective therapy to eliminate bacteria and fungi, even resistant strains, that cause localized infections of the skin and oral cavity [3, 6-8]. This approach combines a photoactive molecule (a non-toxic dye), termed photosensitizer, with visible light and oxygen to produce cytotoxic oxygen species that are able to react with cellular components leading to cell death [3, 9, 10]. Several studies have been shown that the use of the antimicrobial photodynamic therapy (APDT) as a therapeutic approach to treat localized infections is an emerging and promising field [3, 6-8]. Therefore, this dissertation aimed to contribute for the development of an APDT approach against candidosis. The principal aim of this work was to optimize the inactivation of *C. albicans* biofilms by APDT through the action of two new photosensitizers (benzophenoxazinium chlorides of different molecular size) that were synthesized by the Chemistry Department of University of Minho. A set of parameters that guarantees the inactivation of *C. albicans* biofilm cells by APDT was optimized in this work. These parameters include the photosensitizer concentration, the contact time with *C. albicans* biofilms that ensures dye uptake and the light dose that promotes the cytotoxic oxygen species production.

Additionally, it was evaluated the dye uptake during the incubation conditions with the intent to verify if there is a correlation between the APDT outcomes achieved and the levels of dye uptake.

The present dissertation is divided into four chapters. Chapter 1 is an introduction to the theme, where the *C. albicans* characteristics, pathogenicity, virulence factors and its mechanisms of drug resistance, as well as the principles of APDT are described. Additionally, this chapter also shows a short review of the main photosensitizers and light sources used, as well as the potential antifungal applications of APDT. The second chapter includes the materials and methods used during all experimental work. On chapter 3 the results obtained and their discussion are presented. The last part (chapter 4) reveals the main conclusions and presents some suggestions for future works.

Part of the results obtained in this dissertation were presented in the form of Poster in the “2nd Fungal Biofilms Meeting” Conference on May 20th and 21st of 2013 with the following reference: Lopes, Marisa, Alves, Carlos, Rama Raju, B., Gonçalves, S., Coutinho, P., Henriques, M., Belo, I. *Antifungal Photodynamic Efficacy of Benzo[a]phenoxazinium Chlorides against Candida albicans Biofilms*. 2nd Fungal Biofilm Conference, Glasgow, Scotland, 20-21 May, 2013.

1. CHAPTER I

INTRODUCTION

1.1. *Candida albicans*

In nature there is a wide diversity of microorganisms, however only a small part is able to act like opportunistic pathogens and cause infections on human host. *C. albicans* is the most virulent among all the well-known clinically relevant *Candida* species and the species most predominant found on superficial fungal infections of the skin, oral cavity, esophagus, intestinal and genital tract (candidosis), as well as in invasive blood stream infections (candidemia) [3].

C. albicans is a commensal microorganism present in the normal flora of the human body that has an optimal growth at the body temperature (37°C) [11]. Although they are commensals on the majority of healthy individuals, whenever the opportunity arises, i.e, whenever the body is immunocompromised or debilitated in some other way, *C. albicans* becomes a serious pathogenic and opportunist microorganism, causing serious fungal infections. For these reasons, *C. albicans* is not only the main species related with oral mycoses but also the most common fungus affecting HIV infected patients and those with haematologic and oncologic malignancies during the immunosuppression period. In these patients, oropharyngeal candidosis episodes are the most cause of morbidity, which are of special concern, once oral candidosis can lead to esophageal candidosis and even more serious complications [3].

The cell wall of *C. albicans* is an essential component of its success as a pathogen [4]. It is required for growth, provides strength and protection against osmotic insult and establishes the contact between *C. albicans* cells and host tissues, through some associated cell surface macromolecules, leading to tissue invasion and colonization [12]. However, the pathogenicity of *C. albicans* may be attributed to several virulence factors including host defenses evasion, production of some tissue-damaging hydrolytic enzymes, as well as adherence and biofilm formation on host tissues and medical devices [4]. The biofilm formation ability is indeed the main virulence factor of *C. albicans* to the extent that it is the main responsible for its drug resistance against a wide range of conventional antifungal agents, including amphotericin B and fluconazole [4, 13]. Next will be reviewed each of these elements that contribute for *C. albicans* pathogenicity.

1.1.1. The Role of *C. albicans* Cell Wall

The fungal cell wall is a dynamic and highly organized organelle that determines both cell shape and its viability, as well as acts like a permeability barrier and determines the interaction between the microorganism and its environment [14, 15]. Because the fungal cell wall is a dynamic structure, it is continuously biosynthesized and extended during cell proliferation and growth phase. So, although the fungal cell wall has a protective function for cells, it is also responsible for the cell susceptibility to some antifungal agents that have the ability to disturb the processes by which the cell wall is synthesized [16].

C. albicans cell wall is mostly composed by polysaccharides, representing around 80% of the cell wall dry weight. This structure consists in β -(1,3)-glucan covalently linked to β -(1,6)-glucan and chitin and is designed to work as a robust external skeleton, as well as a scaffold for the external glycoprotein layer that represents the other 20% of cell wall constituents. This layer includes not only lipids and various inorganic salts, but also many proteins that are involved in permeability control, interaction with hosts, recognition of other fungi and regulation of several processes [17, 18]. Besides the fungal cell wall being a crucial factor to host tissue evasion and colonization, it is also the first point of contact with innate immune system of the host and thus it also plays an important role in recognition and phagocytosis by host immune cells [15].

1.1.2. Virulence Factors of *C. albicans*

It was believed, decades ago, that yeasts were passive participants of the pathogenesis process and the organic weakness and immunocompromised patients was the only mechanism that triggers the establishment of opportunistic infection. Nowadays, it is known that these microorganisms are active participants in the infection process, using mechanisms of host cells aggression termed virulence factors [4].

C. albicans virulence factors include the ability to express specific host recognition and adhesion biomolecules, secretion of hydrolytic enzymes, morphologic transition between unicellular yeast cells and filamentous phase (hyphae and pseudo-hyphae) and the ability of biofilm formation on several surfaces [4, 11].

The primary factor that contributes to the *C. albicans* virulence is the host recognition and adhesion [4]. These two phenomena are conferred by specialized cell wall proteins termed

adhesins that bind specifically to peptides or sugar residues of other cells and/or increase the cell surface hydrophobicity, promoting the binding to abiotic surfaces through hydrophobic interactions [19]. The mechanisms of adhesion can be divided into two groups: lectin-like adhesion and sugar-insensitive adhesion [19]. The first one refers to lectin-like binding of adhesins to cell surface sugars residues, because these adhesins have a lectin-like carbohydrate binding domain. On the other hand, on sugar-insensitive adhesion, adhesins bind to peptides or raises the hydrophobicity of cell surface promoting the binding to certain abiotic surfaces [20]. One example of the later one in *C. albicans* is the Agglutinin-like sequence (Als) proteins that specifically bind to peptides [21].

One of the most remarkable features of yeast adhesion is the ability to adapt the adhesion properties to new environments [19]. Several signaling pathways are involved in adhesins synthesis in response to stress, nutrient limitation or molecules produced by hosts. These include the Ras/cAMP/PKA, the Mitogen-activated Protein Kinase (MAPK) – dependent filamentous growth and the main glucose repression pathways [22]. Additionally, adhesins are submitted to stochastic expression patterns [23]. These cell wall proteins have a common structure of three domains: the C-terminal that links the adhesin to the cell wall, the N-terminal projected from the cell surface and the middle domain rich in threonine and serine-rich repeats [19]. Because of their similarity and repetitive occurrence, these repeats trigger recombination events and/or slippage during the DNA replication, offering an endless reservoir of adhesion properties to cells that gives them a great opportunity to quickly adapt to stressful environments [23].

The production and release of hydrolytic enzymes, most of them resultant from extracellular secretion, are also a key factor on *C. albicans* virulence [4, 24]. These enzymes help on host adhesion, tissue invasion and destruction, as well as they are also thought to be responsible for changes on host immunity response [4]. The most discussed hydrolytic enzymes released during the pathogenic process are aspartic proteinases (Saps), but phospholipases and lipases are also hydrolytic enzymes that are involved in *C. albicans* virulence [24]. The proteolytic activity of Saps is attributed to a multigene SAP family of, at least, ten members that are differentially regulated and expressed on *C. albicans* infections, suggesting that different Saps have distinct roles during the infectious process [24]. These enzymes are responsible for the digestion or destruction of host cells membrane and degradation of host surface molecules, contributing to host tissue invasion [24]. Additionally, recent evidences have suggested that Saps are also involved in the

activation and maintenance of the inflammatory response in epithelial surfaces [25]. On the other hand, phospholipases are enzymes with the ability to hydrolyse ester bonds in glycerophospholipids [24]. Seven phospholipases have been identified [26] being the difference between their the mode of action and the target within the phospholipid molecule, which is the major component of cell membrane [24]. The functions of phospholipases on *C. albicans* virulence are not yet clear but they have showed to be involved in adhesion to epithelial cells and cell penetration [24] as well as in epithelium invasion [27] and may be in interaction with host signal transduction pathways [27]. Regarding to lipases, they have the ability to catalyse the hydrolysis of the ester bonds of phospholipids and mono- di- and triacylglycerols, but almost nothing is known about their role as *C. albicans* virulence factor. The potential roles of lipases that have been suggested include the digestion of lipids for nutrient acquisition, lyses of competitive microflora, adhesion to host tissues, as well as changes in immune cells [28, 29]. In addition, the production and release of haemolysins may also play a key role in *C. albicans* virulence [4]. *C. albicans* expresses haemolysins that allows the destruction of red blood cells and the acquisition of iron from host erythrocytes, an essential element for the development of microorganisms and a consequent establishment of infection [30].

The ability to go under a reversible morphologic transition between unicellular yeast cells and filamentous phase (hyphae and pseudo-hyphae) is another important virulence factor of *C. albicans*, with the extent that this ability provides cells with a flexibility of adaptation to hostile conditions imposed by the human body [4]. The filamentous phase raises resistance to phagocytosis and it has a cell wall containing three times more chitin that gives it more mechanical strength and makes epithelium penetration easier, allowing the invasion of more deep tissues [4, 31]. Although the parameters that triggers morphologic transition are not yet well understood, *in vitro* studies show that this behavior is influenced by temperature and pH: unicellular phase are stimulated at 25°C and acid pH, whereas filamentous phase is favored at 37°C with pH around neutrality [11].

The most important virulence factor of *C. albicans* is the capacity to form biofilm on several surfaces [4]. Recent evidence suggests that the majority of *C. albicans* infections are associated with biofilm formation [13]. In fact, *Candida* species, most notably *C. albicans*, are the main fungal species associated with biofilm formation causing superficial and deep-seated infections. This microorganism can colonize not only epithelial surfaces, but also numerous medical devices

(e.g. catheters and prosthetic devices, like voice prostheses, heart valves, denture surfaces and etc.) [3, 32].

Biofilms are defined as highly well structured, coordinated and functionalized communities of microorganisms that are surface associated or attached to one another and embedded in a self-produced protective extracellular matrix (ECM) composed by diverse polymeric substances such as cell wall glycoproteins and polysaccharides (e.g. β -glucan) [4, 13, 33]. Fungal biofilms have defined key phases of development that were elucidated through the use of model systems. These key phases include the arrival to the substratum, adhesion, colonization, ECM production and deposition, biofilm maturation and cell dispersal [13]. Figure 1 shows the steps in *C. albicans* biofilm formation.

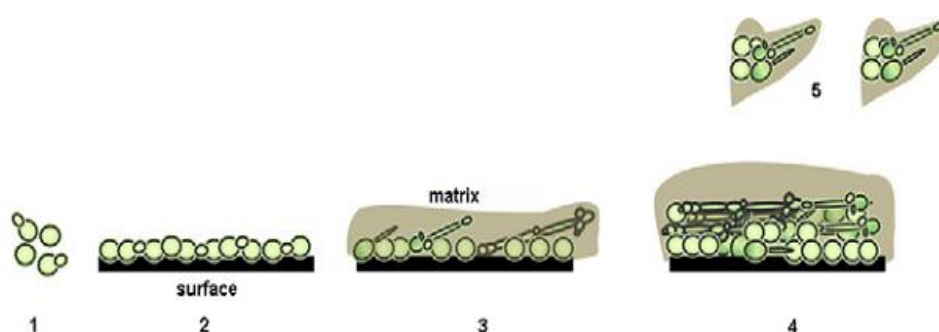


Figure 1. Illustration of steps in *Candida albicans* biofilm formation. 1 and 2. Formation begins with adhesion of yeast cells to a surface by nonspecific interactions, such as hydrophobic and electrostatic forces, as well as specific adhesin-ligand bonds. 3. Attached cells proliferate to form microcolonies and start to deposit the ECM. 4. The biofilm grows into a thick layer where ECM involves a complex network of yeast cells, hyphae and pseudohyphae. 5. Cells released or detached from the biofilm spread into the environment, dispersing infections and forming new biofilms. Adapted from [3].

The advantages to an organism of forming biofilms include the protection from the environment, resistance to chemical and physical stress, regulation of gene expression and metabolic cooperation [13]. Usually, the metabolic activity of biofilms is lower than planktonic cells due to existent nutritional restrictions, environmental physical stress and high cell population. These communities also show unique phenotype characteristics compared to their planktonic counterparts that confer them an increased resistance to antifungal agents [13, 34-36]. In the clinical scenario, the problematic of drug resistance is very important since it enables biofilms to act as persistent sources of infection [13].

1.1.3. The Role of Biofilm in Antifungal Agents Resistance

The increased resistance to antifungal agents is one of the defining characteristics of biofilms [13]. Nowadays, *C. albicans* biofilms show an increased resistance to a wide range of conventional antifungal agents, such as amphotericin B and fluconazole. This phenotype can be about twenty times more resistant to amphotericin B and one hundred times more resistant to fluconazole than the planktonically growth form [3, 37].

Antifungal resistance is both complex and multifaceted. The resistant phenotype of planktonic cells is generally due to irreversible genetic changes, but biofilms are able to be resistant through their physical presence and cell density, which turns it into an almost inducible resistant phenotype independent from the genetic alterations [13]. Understanding the processes mentioned above enabled the science to unravel the mechanisms that are involved in drug resistance. Over the last few years, several factors that play a role in fungal biofilm resistance have been described, including the physiological state, cell density, extracellular matrix, efflux pump-mediated resistance, overexpression of drug targets and the presence of persister cells [4, 13, 38].

The general physiological state of cells in sessile populations are implicated on the susceptibility profiles of fungal biofilms [13]. Nutrient and oxygen limitation, particularly in the deeper cell layers of the biofilm, are responsible for slowing down the growth rate of these cells leading to cell's surface alterations that consequently would result on a slower or inefficient drug uptake [34, 35, 39]. However, other factors like pH, temperature, changes in osmolarity, oxidative and ionic stress can also cause stress responses through conserved signaling pathways and perhaps alter their antifungal susceptibility, which suggests that more complex factors may be involved on drug resistance of biofilms [40, 41]. Some of the most tolerance responses triggered by these physiological stress factors is the activation of MAPK signal transduction network that is involved on biofilm development [22, 40], the activation of the Calcineurin via that plays among other things an important role on antifungal drug responses [42, 43] and finally the activation of the heat shock protein (HSP) Hsp90 that regulates complex cellular circuitry and potentiates the resistance to azoles and echinocandins in *C. albicans*, at least through the calcineurin via [44].

Cell density is also an important resistance factor of biofilm populations [13]. A previous investigation showed a phase-dependent increased antifungal resistance on the biofilm

development, supporting the belief that the physical density of cells within biofilms plays a role in drug resistance [45]. Within these highly dense communities there is a cooperation between cells through the quorum sensing systems, which enables them to promote communication and collective behaviors via the secretion of signaling molecules in a population-dependent manner [46]. This process allows communities to improve nutrient and niches accesses, as well as, collective defense against other competitive microorganisms and antifungal agents [3, 4]. However, some previous work have shown that both planktonic and biofilm resuspended cells shows similar resistant phenotype to the Clinical and Laboratory Standards Institute (CLSI) methodology, suggesting alternative mechanisms of resistance [47].

The ECM is an important feature of biofilms with the extent that this component provides to cells protection from host immunity and antifungal agents [48]. Its principal role in the antifungal resistance is the diffusion barrier effect that restricts drug diffusion throughout the biofilm structure, particularly to the deeper cell layers, and therefore, only the most superficial layers are exposed to lethal doses of antibiotics [35]. Recently, it was also been shown that the ECM composition of *C. albicans* biofilms have also a central role in drug resistance. In this respect, some recent results have shown that β -1,3 glucans are responsible to sequestering azoles and thus conferring resistance on *C. albicans* biofilms [49]. Additionally, the regulation of ECM production may also be a key resistance factor [13]. It is thought that some glucoamylases and alcohol dehydrogenases may have positive roles on the matrix production and maturation phase of biofilms, respectively [50].

The fungistatic effect of the azoles against *C. albicans* induces a strong response of the biofilm population, allowing the development of some drug resistance mechanisms [13, 51]. The principal molecular mechanism of azole-resistance in *C. albicans* is the increased efflux of antifungal agents principally mediated by the Adenosine Triphosphate (ATP)-binding cassette and major facilitator superfamily (MFS) transporters [4, 45, 52]. The increased drug efflux by ATP-binding cassette (ABC) transporters is due to the overexpression of the genes encoding drug efflux pumps *CDR1* and *CDR2*, whereas the contribute of members of the MFS on azole-resistance is mostly due to the overexpression of the *MDR1* gene, a gene that encodes drug efflux pumps of MFS [45, 52, 53]. In fact, efflux pumps are an important determinant of fungal biofilm resistance. Their primary role may be the protection of cell to acute toxicity, but a clinical

exposure to azoles may triggers the levels of efflux pump expression and thus contributing for drug resistance [54].

Ergosterol alterations in biofilm cell membranes may also be the reason for *C. albicans* resistance to both azole and polyene-derived antifungal agents [45, 52]. Azoles actively bind to ERG11p enzyme (lanosterol 14-a-demethylase) encoded by *ERG11* gene and block ergosterol biosynthesis, leading to a depletion of cell membrane ergosterol and the accumulation of toxic sterol pathways intermediates capable to inhibit cell growth [40, 55]. On the other hand, polyenes use the binding to cell membrane ergosterol to promote the formation of cell membrane pores and consequently cause the loss of intracellular substances, leading to cell dead [56]. Thus, amino acid substitutions in the enzyme ERG11p due to missense mutations on *ERG11* gene or the overexpression of this enzyme may cause ergosterol alterations that elicit azole and polyenes resistance on *C. albicans* [55, 56]. It has been reported that mature *C. albicans* biofilms show an overexpression of the enzyme Erg11p, as well as a significant content of altered membrane ergosterol [3, 45].

The presence of persistent cells (0.1-1% of biofilm population) is also one important mechanism of resistance in chronic infections that has gathered some recent attention in fungal biofilms [13, 57]. Persister cells are “dormant variants of regular cells that form stochastically in microbial populations and are highly tolerant to antibiotics” [58]. In particular for *C. albicans* biofilms, it has been described the presence of a small subpopulation of yeast cells that are highly resistant to amphotericin B, independently of efflux pumps upregulation or cell membrane composition [4, 13, 59]. It is thought that phenotypic adaptive changes arising from the prolonged and ineffectual antifungal treatment may be the responsible for the extraordinary survival ability of persister cells and thus for the antimicrobial drug failure [13]. However, the exactly mechanisms that enable these subpopulations to persist still remain unclear.

The antifungal biofilm resistance seems to be a multifactorial and complex process, where antifungal agents with a single mechanism of action are likely to be poorly effective. Thus, other antifungal strategies with more effective mechanisms of action are needed [3, 34].

1.2. ANTIMICROBIAL PHOTODYNAMIC THERAPY (APDT)

The deadly effect of visible light when combined with chemical compounds was described for the first time by Oscar Rabb and his professor Herman Von Tappeiner in 1900. They found that visible light combined with acridine was able to inactivate cultures of *Paramecium caudatum* [14]. Shortly later, the essential role of the oxygen and light in the process was demonstrated by Von Tappeiner, who created the term “*Photodynamic*” [6]. However, the potential of PDT against pathogens was not explored over several years for two principal reasons: some pathogens, especially gram-negative bacteria and protozoa, are poorly inactivated by PDT and the discovery of antibiotics, particularly the penicillin in 1928, raised the belief that every microbiological diseases would have been reduce to a level that nevermore would have impact on human health [14]. Such expectations were disappointed in the end of 50 decade with the emergence of resistant strains and then, the researches on the PDT approach were retaken [6, 14].

In the 70s, it was discovered that porphyrins dyes localized selectively in tumors and so, PDT was initially developed as a cancer therapy. Since then, PDT has been clinically used for therapy of various diseases. So far, PDT is approved by FDA (Food and Drug Administration) for treatment of non-melanoma skin cancer (basocellular carcinoma and Actinic Keratosis), choroidal neovascularization in age-related macular degeneration, as well as in treating lung and Barrett's esophagus cancer [10, 60, 61]. On the other hand, PDT investigations has included a wide range of applications, such as arterial restenosis prevention, therapy of another malignancies (prostate, neck, mesothelioma and brain) and autoimmune diseases, such as psoriasis [60, 61].

Recently, antimicrobial PDT (APDT) has been proposed as an alternative approach to kill pathogens. APDT combines a non-toxic and light sensitive dye, termed photosensitizer, with oxygen and harmless visible light with appropriate wavelength, which matches with the absorption spectrum of photosensitizer [61-63].

Initially, this therapy requires a localized administration of the photosensitizer. Then, the photosensitizer taken up by cells or attached to them is excited with the visible light source, by photon absorption. On this state, the photosensitizer can undergo reaction with ambient oxygen and could originate cytotoxic oxygen species that may kill pathogens by oxidative modifications of the cellular constituents [14, 62, 64, 65].

1.2.1. Photophysical processes of PDT

The photosensitizers used on this therapy are molecular structures characterized by conjugated double bonds containing a system of π -electrons. In the photosensitizer ground (singlet) state these electrons are spin paired at the low energy orbitals. Upon application of the light with wavelength corresponding to the absorption peak of the photosensitizer, the electron in the highest occupied molecular orbital (HOMO) is excited to the lowest unoccupied molecular orbital (LUMO) and keeps its spin, leaving the photosensitizer in the excited singlet state, which is highly unstable and short lived (in the range of nanoseconds) [62, 66]. At this phase, the photosensitizer can rapidly return to the ground state, releasing the energy absorbed as fluorescence or suffering internal conversion, releasing heat. However, the most important event to the photodynamic therapy is the reversal of the excited electron's spin, known as intersystem crossing, which leads the photosensitizers to the triplet state. This state is less energetic than the previous state, but has a longer life time (in the range of microseconds) [64, 65].

In the triplet state, the photosensitizer may return to the ground state once again, by a newly change in the excited electron's spin orientation followed by energy emission as phosphorescence or, alternatively, the photosensitizer may interact with molecules in its immediate environment (essentially with molecular oxygen, O_2) according two type of mechanisms: type I and type II reactions (Figure 2)[62, 64, 65].

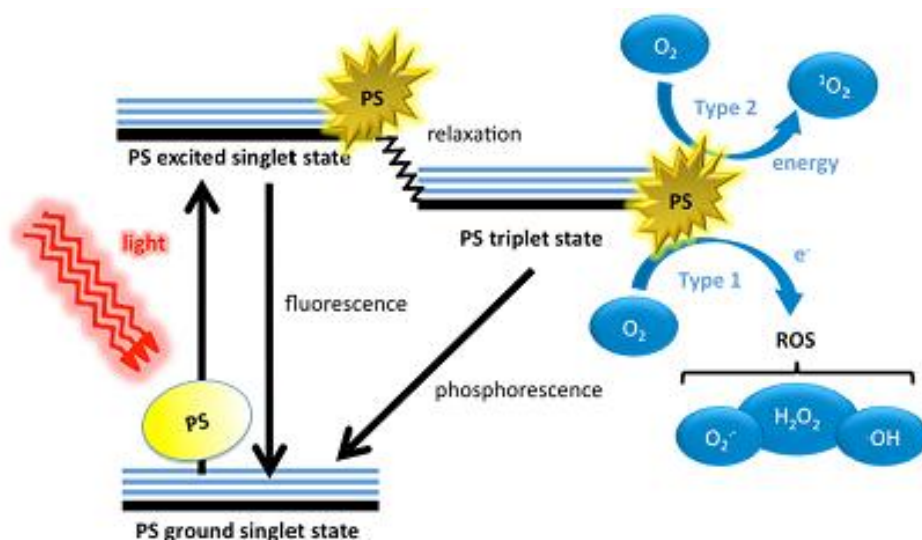


Figure 2. Schematic illustration of photodynamic therapy mechanism of action. Adapted from [62].

Type I Reaction

On the type I reaction, the triplet photosensitizer can transfer an electron and sometimes a simultaneous proton to O_2 , resulting on superoxide anion ($O_2^{\bullet-}$) formation, which may undergo reaction and originate other reactive oxygen species (ROS), including the hydroxyl radical ($\cdot OH$) and hydrogen peroxide (H_2O_2) [62, 64].

The ROS formed have a range of different reactivities. $\cdot OH$, a strong electrophile that has the ability to chemically cause damage to a wide range of molecules, is undoubtedly the most reactive. H_2O_2 shows a less reactivity and $O_2^{\bullet-}$ is the least reactive [67]. However, $O_2^{\bullet-}$ may be converted to H_2O_2 and O_2 by the superoxide dismutase enzyme. H_2O_2 is really reactive in the presence of ferrous irons and so, it may undergo reaction leading to $\cdot OH$ formation, through the well-known Fenton reaction (equation 1) [62, 66].



More specifically, in the Fenton reaction occurs the homolytic fission of the oxygen-oxygen bond in H_2O_2 molecule, resulting in OH^- and $\cdot OH$ formation, through the oxidation of ion Fe^{2+} to Fe^{3+} [68].

Type II Reaction

The electronic structure of O_2 in the ground state is a triplet. In other words, in the ground state, the O_2 molecule has two outermost orbitals unpaired but spin parallel [64]. As the O_2 ground state and the photosensitizer excited state is the same (triplet state), the collision between these two molecules can undergo energy transfer, transforming O_2 in a more oxidant specie. In a detailed way, type II reaction involves energy transfer to O_2 , resulting in a spin reversion of its outermost electron and its shifting into the orbital containing the other electron, leaving one orbital completely unoccupied. As a result, the termed singlet oxygen (1O_2) is formed and photosensitizer returns to the ground state [9, 62].

Singlet oxygen is highly reactive, very short lived (around microseconds), due to its very instable electronic configuration, and has a very limited diffusivity. Its high reactivity is responsible for a central role in the cellular damages during the photodynamic therapy and the

limited diffusivity gives it a simultaneous localized effect (in a radius of approximately 20 nm) [60, 62, 66].

Although both types of reactions can occur simultaneously in the presence of molecular oxygen, the second one occurs preferentially. Thus, singlet oxygen is not only more reactive than ROS, but also the main product of the photodynamic process, constituting the principal responsible for causing cellular damages [67].

1.2.2. The Photobleaching Process

As a consequence of light exposure, the photochemical destruction of the photosensitizer can occur. This process called photobleaching is generally denounced by the decrease of photosensitizer's fluorescence intensity over time and can be minimized by decreasing illumination light intensity [66].

It was thought that the photobleaching process is due to a reaction between the photosensitizer molecule and singlet oxygen or ROS produced during illumination in a way that leads to a decrease of its efficacy for further photosensitization processes. However, in some cases the first product of photobleaching is a better photosensitizer than the initial molecule [66].

Photobleaching generally means a loss of reactivity but this process can have some beneficial effects towards selective treatments. In fact, it is thought that photobleaching may be responsible for the destruction of large amounts of photosensitizers on healthy tissues [69]. If this process occurs fast enough, healthy tissues may be spared from photodynamic cell damages, increasing injury site selectivity. However, there are still no clear evidences that the photobleaching can affect PDT treatments in this way [66, 70].

1.2.3. Mechanism of Action of APDT

The APDT Mechanism of action is quite different depending on the type of target microbial cells. The pathway where an initial increase of permeability of the cell wall is required, being an operative pathway for yeasts and also for gram-negative bacteria and protozoa in the cystic stage will be described [14].

The process begins when the photosensitizer (positively charged) binds to negative charges of the cell wall, according to electrostatic forces. Then, this agent can modify the cell wall

permeability (in the dark or photo-induced), leading to a massive influx of the photosensitizer for the plasma membrane [14, 71]. At this point, a portion of the photosensitizer may cross the plasma membrane and take different subcellular localizations, especially when a prolonged incubation period is used. In the last few years, some authors have been described that certain photosensitizers can cross the plasma membrane of eukaryotic cells and accumulate in mitochondria, lysosomes (vacuoles, in the case of fungi) or Golgi apparatus, as well as in endoplasmic reticulum [66].

Upon illumination, the reactive cytotoxic species formed will oxidize the diverse cellular constituents within the microenvironment of the photosensitizer, affecting the cell functions and its metabolism in a manner that it can result in cellular apoptosis or necrosis [3, 14]. The mechanism of action that leads to fungi inactivation by APDT is illustrated in Figure 3.

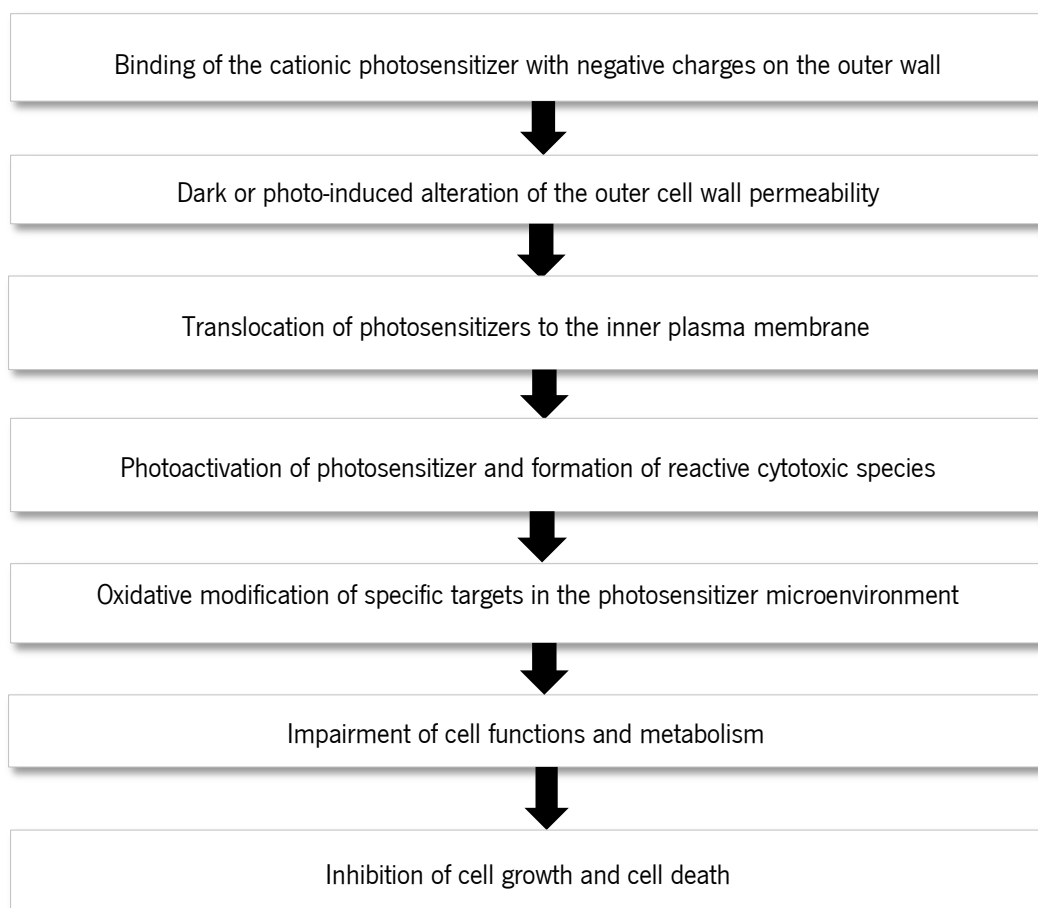


Figure 3. Illustrative scheme of essential steps involved on antifungal photodynamic therapy. Modified from [14].

As mentioned above, the cytotoxic effect of singlet oxygen is the most responsible for cellular inactivation. Singlet oxygen has a high probability to react with sulfur moieties and double

bonds, having the ability to interact with aromatic components of macromolecules [62]. Thus, this product of type II reaction is a non-specific oxidizing agent that has multiple targets. It has the ability to oxidize aminoacids, inactivating some proteins and enzymes (e.g., catalase, superoxide dismutase, alcohol dehydrogenase, cytochrome coxidase, glyceraldehyde-3-phosphate dehydrogenase and hexokinase), as well as it is responsible for oxidation of nucleic acids and lipids peroxidation [9, 72]. In particular, lipids peroxidation can lead to the lyses of vacuoles, mitochondria and plasma membrane [3].

Mitochondria are an important target of APDT. APDT induced mitochondrial damages have been related to the tendency of many photosensitizers to produce cell apoptosis involving the caspases pathway or the release of cytochrome c [66, 71]. However, plasma membrane represents the critical target of APDT. The damages caused on this organelle can lead to loss of barrier properties and inhibition of calcium and potassium transporter proteins, resulting in cell swelling, loss of cellular constituents, collapse of cell ionic balance, as well as deficiency of some essential substrates of anabolic and catabolic pathways [14, 73]. Additionally, the damage caused in the cell wall and plasma membrane may allow more photosensitizer to be translocated to endocyttoplasmic districts and produce more reactive cytotoxic species upon illumination that will cause more oxidative modifications on a variety of cell targets [3, 66].

Although singlet oxygen can react with nucleic acids, several studies shown that the oxidative damages caused on plasmid and genomic DNA are not directly correlated with cell death [14, 74, 75]. In fact, DNA photo-induced oxidative modifications are little significant, since (i) the bacteria *Deinococcus radiodurans*, which has a highly efficient mechanism of DNA repairing, is quickly killed by APDT [14]; and wild strains of *Escherichia coli* have similar sensitivity to inactivation by APDT than *E. coli* strains with deficient DNA repairing mechanisms [76]. These observations are in agreement with the lack of mutagenic effects observed in photosensitization of microbial cells with several photosensitizers [14].

1.2.4. Biofilms Eradication by APDT

The clinical significance of biofilms is highlighted by recent estimates that over 65% of all hospital infections are originated by these microbial communities [41, 57]. A recent scanning electron microscopy studies [77, 78] have provided evidences that APDT has not only the ability to kill a wide of pathogens within the biofilm but also has a direct effect on biofilm extracellular

biomolecules. These authors described that the high reactivity of singlet oxygen exerts also effect on the matrix polysaccharides, leading to biofilm destruction [3]. This twofold activity of APDT in biofilm eradication may be very advantageous in clinical use because the structural rupture of biofilms may inhibit plasmid exchanges and transference of drug resistance factors, as well as may avoid new colonization and prevent recurrent infections [9]. However, there are only a few studies in this area and most of them were developed using biofilms of pathogenic bacteria. Given the high clinical relevance of fungi and fungal biofilms, there is a substantial need to provide a deep understanding about the APDT effect on these communities.

1.2.5. Cellular Resistance Mechanisms to APDT

Since APDT products have no specific target and can cause damage to a variety of cellular constituents, it seems to be very unlikely that microbial cells can develop resistance to APDT [3].

One mechanism that may provide cellular resistance to APDT is the inactivation of the oxygen reactive species H_2O_2 , $\cdot OH$ and $O_2^{\cdot -}$ by antioxidants detoxifying enzymes, such as catalase, superoxide dismutase and peroxidase [62, 79]. For instance, the catalase enzyme can remove the hydrogen peroxide (H_2O_2) from the Fenton reaction on type I process, breaking down this molecule and forming water (H_2O) and oxygen (O_2) [80]. In addition, some antioxidants peptides, such as glutathione, may also quench some oxygen reactive species leading to the development of cellular resistance to APDT [62]. On the other hand, singlet oxygen cannot be broken down by antioxidant enzymes in any enzymatic reaction, by contrast it has sometimes the ability to inactivate them, which is the case of catalase and superoxide dismutase [81].

It was also thought that the general mechanisms of cell drug resistance, such as active efflux pumps, altered drug uptake and intracellular trafficking of the photosensitizer may contribute to the microbial resistance to APDT [3]. In the particular case of *C. albicans*, it has been shown that the two major efflux systems, ABC and MFS transporters, are responsible for the decrease of the killing effect of methylene blue (MB) – mediating APDT against this pathogen, which suggests that both type of transporters are involved in MB efflux. To overcome this problem, some authors proposed the combined use of efflux pumps inhibitors [3, 77]. However and according to Prates et al. [82], the phototoxic effect of MB is improved using an ABC transporter inhibitor, but is decreased when a MFS channel inhibitor is used, suggesting that

MFS channels are also an uptake mechanism of MB [82]. Nevertheless, some authors support that photosensitizers have not to be necessarily taken up by cells. The main important cellular targets of APDT are the cell wall and plasma membrane and so, photosensitizers that specific bind to these cell structures will be potential photosensitizers for APDT of the target cell [3].

On the other hand, some recent studies [79, 83] have revealed that the expression of HSP can be significantly increased after the photodynamic treatment. These proteins play an important role in refolding proteins and prevention of protein aggregation. So, it may constitute a mechanism whereby microbial cells could develop resistance to APDT. For instance, in 2011 St Denis et al. [63] had demonstrated that APDT-mediated by Toluidine Blue (TBO) in *E. coli* and *Enterococcus faecalis* leads to the upregulation of the HSPs DNaK and GroEL and consequently its survival is increased in about 2 log and 4 log, respectively. However, the mechanism that leads to HSP expression is no yet completely understood and the combination of APDT with HSP inhibitors does not seem to potentiate the killing effect of APDT in both microorganisms [3].

In summary, the studies and reports discussing the possible microbial resistance to APDT are scattered and sometimes are quite controversial. Thus, a better knowledge in this field is needed and perhaps could provide new therapeutic approaches, such as the combination of APDT with other therapies [3].

1.2.6. Applications of APDT

The APDT potential have been investigated in a wide range of applications. Given that photosensitizers have a broad antimicrobial spectrum of action, their use as general disinfectants have been studied. This approach could be used to sterilize chirurgic material, blood products and also surfaces and floors of wards or other healthcare facilities. On this last application, photosensitizers could be applied as a wash liquid or spray and illuminated using ambient lights, that will induce the production of oxygen cytotoxic species and so, an antimicrobial effect that could lead to a decrease of the amount of microbial transmission in these places without induces drug resistance to the conventional drugs [9].

On the other hand, applications like the sterilization of oral cavities and root canals, as well the treatment of localized infections (e.g. impetigo, candidosis and periodontitis) seems to be also a promising feature of APDT [6, 14, 60]. Besides these sites are readily accessible to topical delivery of photosensitizers and light, this therapy may also kill the resistant strains without arm

the surrounding tissues. Indeed, there is a possible set of optimal conditions that makes APDT suitable to treat localized infections [14]. The combination of an appropriated incubation time, low photosensitizer concentration and slight illumination parameters appears to allow a selective killing of pathogens, sparing human cells (e.g., keratinocytes and fibroblasts) from photo-induced cell damages [84-86]. Therefore, APDT provide a good antimicrobial alternative approach that may decrease the mortality rates of the microbial associated diseases [3].

With the respect to photodynamic inactivation of *C. albicans*, superficial and localized infected tissues on the skin and mucosae, such as mucocutaneous candidosis, seems to be the main application of antifungal PDT [5]. Several classes of photosensitizers, mostly belonging to the phenothiazines and porphyrin classes have been used on APDT of *Candida* species growing on both planktonic cultures and biofilms (see section 1.3.2.) [3]. Many in vitro studies have been reported the use of APDT on killing *Candida* species and some in vivo studies have also been developed [7, 87-101].

1.3. PHOTSENSITIZERS

In the last 30 years, the research on APDT field has significantly increased and thus, several forms of photosensitizers have been created. Photosensitizers are organic aromatic molecules constituted by large conjugated systems of double bonds that can be considered as a central cromophore combined with auxiliary side chains that are responsible for further electron delocalization of the photosensitizer [14, 62, 65]. Although APDT success is influenced by oxygen availability and illumination light dose, photosensitizer concentration, as well as its own properties are crucial parameters on the photodynamic inactivation process of pathogens [3, 65, 67].

1.3.1. Properties of Photosensitizers

The type and efficacy of cellular mechanisms of uptake of dye, as well as the pattern of its distribution into the cell are dependent on its chemical properties, such as the amphiphilic character, lipophilicity-hidrophilicity balance, degree of ionization or the presence of electric charged groups [5].

In particular, the amphiphilic character and the presence of electric charged groups are very important factors on photosensitizer performance. While amphiphilic property avoid self-aggregation of photosensitizer and provides a good penetration in the lipid layer of plasma membrane, the presence of electric charged groups provides electrostatic affinity that encourages the distribution of photosensitizer for various subcellular targets [5, 66, 102]. However, there are small details to consider depending on the target. Some photosensitizers that are efficient in killing gram-negative and gram-positive bacteria do not show the same therapeutic effect in fungi. For instance, a large number of positive charges are required to inactivate bacteria, but the same structural factor does not provide a good binding or uptake by fungi cells, especially if they are distributed homogeneously. In this case, more lipophilic structures with less positive charges seem to be more appropriated [62].

Although there are small differences between suitable photosensitizers for fungi or bacteria, there is a consensus on the electronic character of photosensitizers. Cationic structures are more effective to kill both bacteria and fungi than anionic or neutral ones, due the electrostatic affinity provided between its positive charges and the negatively charged groups of cell wall and plasma membrane [14].

Recently, it was also established that there are essential photophysical and photochemical parameters that determine photosensitizing capability of a compound. These parameters are the absorption peak wavelenght (λ_{max}), extinction coefficient (ϵ), triplet-state life time (τ_t), triplet-state quantum yield (Φ_t), triplet-state energy (ΔE_t) and singlet oxygen quantum yield (Φ_Δ), which are all specific of each photosensitizer and dependent on its molecular structure [5, 65]. In short, a photosensitizer with optimal properties to APDT clinical use must have a wide range of properties. Table 1 describes the profile of an ideal photosensitizer for APDT use in the clinical field [5, 14, 64, 65, 70, 102].

Table 1. Profile of an ideal photosensitizer for APDT use in the clinical field [5, 14, 64, 65, 70, 102].

Characteristics	Description
Absorption peak	Absorption in the long-wave region (>630 nm), preferably at a near red wavelength of the visible spectrum makes tissue penetration easier and avoids generalized photosensitization by sun light (400-600 nm).
Extinction coefficient	High extinction coefficient of photosensitizer is required to increase the number of photons absorbed. Strong absorption of the light decreases the amount of photosensitizer required for a certain effect.
Dark toxicity	Low dark toxicity of photosensitizer is desired in APDT clinical use.
Energy transfer and quantum yields	The energy transferred to O ₂ during the photophysical process of APDT must be sufficient to induce singlet oxygen formation. On the other hand, high quantum yield of the triplet-state, combined with high triplet life-time ($\tau_t > 100 \mu s$) and a high quantum yield of singlet oxygen is desired;
Selectivity	Selectivity to microbial cells is desired in the clinical field of ADT.
Stability	Photosensitizers must be stable enough to avoid degradation products. It also should not self- aggregate in the body because aggregates decrease the triplet-state and singlet oxygen quantum yields.
Tolerability	The damages caused on healthy tissues should be minimal.
Pharmacokinetics	Rapid removal from treated tissues and human body is required to avoid generalized photosensitization of the skin.
Broad spectrum of action	Photosensitizers should have a broad spectrum of action allowing the therapeutic of localized infections caused by a heterogeneous microflora of pathogens.
Mutagenicity and resistant strains selection	Photosensitizers should not induce genetic alterations. It should also minimize the risk of resistant strains selection.
Availability	Photosensitizers should be a simple formulation with easy chemical synthesis and its starting materials should be readily available. Moreover, it should be easily produced in large-scale to make it cost-effective and widely available.
Chemical structure	Chemical structures of new photosensitizers should be deviations of other existent photosensitizers, allowing the improvement of its properties.

1.3.2. Most Common Photosensitizers in APDT

The first generation of photosensitizers emerged in 1960 and comprised hematoporphyrins (Hp) and hematoporphyrin derivative (HpD), which is composed by monomeric and oligomeric porphyrins derived from human blood. Although its photosensitizing potential, both Hp and HpD were not suitable for APDT use [65]. Besides its exactly composition was unknown, its characteristics and distribution differed from preparation to preparation (which makes impossible to predict the therapeutic effect), the absorption spectrum (400-600 nm) was less than that idealized for APDT use and the phototoxic effect were mainly promoted by unbounded molecules in the bulk aqueous solution leading to a mediocre killing effect [5, 65, 102].

The second generation of photosensitizers was developed to fill the gaps of first generation. This new photosensitizers have longer wavelength absorption peaks (600-800 nm), that allows a deeper penetration of light in tissues (2-3 cm), reasonable stability, absent or low dark toxicity and good capability to induce singlet oxygen formation [65, 102]. There are numerous classes of photosensitizers belonging to this generation, which were firstly created for the antitumoral application of PDT. However, some of these agents have been also showing efficiency on APDT applications. Porphyrins, phthalocyanines and phenothiazines dyes are the most common photosensitizers used on APDT field (Figure 4) [5, 64, 103].

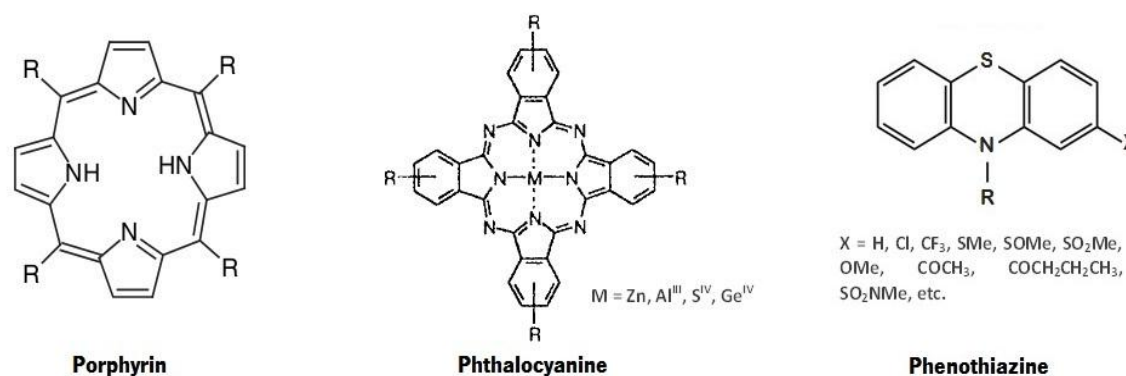


Figure 4. Chemical structures of the main photosensitizers used on PDT. Modified from [14, 102, 104]

Porphyrins

Porphyrins of second generation are pure synthetic molecules that have a central structure composed by tetrapyrrole conjugates, generally associated with various polar hydrophilic

substituents groups: hydroxy, carboxy, quaternary ammonium, sulfonic or pyridinium. These photosensitizers have absorption peaks in the 650 - 700 nm waveband and are 30-times more efficient than HpD. [5, 102].

The polarity of these molecules is their critical factor. The more recent porphyrins derivatives are amphiphilic and water soluble molecules that are characterized by a greater uptake and, consequently, have a better activity against yeasts in comparison to HpD or other porphyrins derivatives [5]. In fact, a new cationic porphyrin photosensitizer - the meso-tetra (N-methyl-4-pyridyl) porphine tetra tosylate (TMP-1363) - was shown highly effective in APDT against yeast forms of *C. albicans* and *C. glabrata* [62]

As microorganisms self-produce and accumulate porphyrins, it has also been adopted the endogenous photosensitization of microbial cells through administration of a small non-dye aminoacid (5-aminolevulinic acid; ALA) [62, 105]. On this approach, exogenously supplied ALA enters into the microbial heme synthesis pathway, allowing an excessive accumulation of protoporphyrin IX (Pp IX). Upon illumination, Pp IX can act like an effective photosensitizer and produce photodamage at the mitochondria level (where it is synthesized), as well as on plasma membrane. Pp IX has its absorption peak at the 375-405 nm waveband, however it has other lowest peak at 630-633 nm region [5, 64, 106].

Phthalocyanines

Phthalocyanines have similar chemical structures to porphyrins and are characterized by the condensation of benzene rings with pyrrole moieties. Chemical properties of phthalocyanines may be adjusted by modifying the central metal/semi-metal atom or the number and type of side chains. In fact, the central atom (Zn , Al^{III} , Si^{IV} ou Ge^{IV}) plays an important role on the phototoxic activity. It may affect the triplet-state life time and quantum yield, as well as the introduction of polar substituents on side chains, which will influence the polarity balance and, consequently, the cell uptake and its distribution into microbial cells [5].

Phthalocyanines have great singlet oxygen quantum yield and high extinction coefficient in the far red (680-720 nm). Despite the lack of knowledge about the phthalocyanines cell targets, they have showed to be effective against *C. albicans*. One recent photosensitizer of this family, BAM-SiPC (also known as *malachite green*), has been shown a great activity against some

pathogens by APDT, including *C. albicans* [62]. Moreover, other study conducted by Lam et al. [94] showed that phthalocyanine PC4-mediated APDT can induce apoptosis of *C. albicans* cells.

Phenothiazines

Phenothiazines have a very dissimilar chemical structure in comparison to all dyes mentioned above. These dyes have simple planar and tricyclic skeleton combined with polar substituents (side chains), having its absorption peak in the 600-900 nm waveband [5, 103]. The most frequent used phenothiazines derivatives are MB and TBO, two efficient producers of singlet oxygen that have its absorption peak at 656 nm and 625 nm, respectively [5, 64].

In yeasts, phenothiazines tend to accumulate on plasma membrane and damage it after light exposure. Both MB and TBO have been shown efficient photosensitizers to *C. albicans* photoinactivation by APDT [5]. In particular, MB and its analogues show killing rates 18-200 times bigger than those determined for keratinocytes, suggesting that MB-APDT of fungal infections of the skin can be highly effective and selective [5].

1.3.3. Benzo[*a*]phenoxazines

Phenoxazines have a similar chemical structure of phenothiazines with the difference that has an oxygen atom replacing the sulfur atom (Figure 5A). Benzophenoxazines are the result of addition of benzene rings to phenoxazines and thus, they may have linear, (benzo[*b*]phenoxazine) or angular structures (benzo[*a*]phenoxazine and benzo[*c*]phenoxazine), depending on orientation of benzene ring fusion. Despite there are three types of structures, only benzo[*a*]phenoxazines have been molecules of interest and widely explored in contemporary science [104]. The presence of substituents groups in some orientations of these structures may give it the ability to freely donate and/or accept electron density, granting them the capacity to emit fluorescence and so, some benzo[*a*]phenoxazines have been widely used as biomolecular probes of DNA and RNA in fluorescence studies [104].

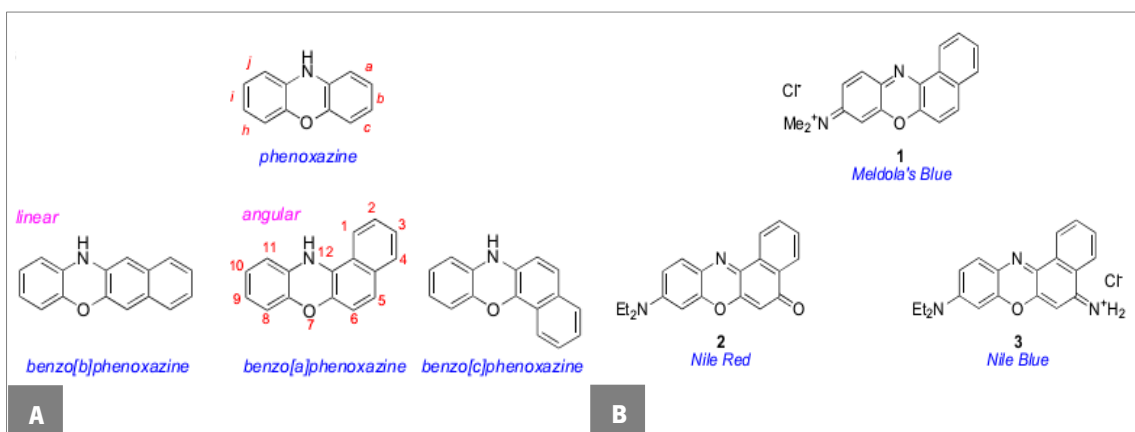


Figure 5. (A) Chemical structure of phenoxazines and benzophenoxazines; **(B)** Structures of the three best known benzo[*a*]phenoxazines. Adapted from [104].

The first benzo[*a*]phenoxazine to be discovered was Meldola's Blue, however Nile Blue and Nile Red are by far the more used (Figure 5B) [104]. As Meldola's Blue is poorly water-soluble and Nile Red is a neutral benzo[*a*]phenoxazine (and so, also poorly water-soluble), the positively charged benzo[*a*]phenoxazine Nile Blue is the only one of interest for APDT [103, 104]. Nile Blue, which has its absorption peak localized at 635 nm, has a positively charged and oxidized phenoxazine system, i.e, it is a benzo[*a*]phenoxazinium dye and has a 9-diethylamino substituent to donate electron density across the ring and an iminium substituent to act as acceptor [104].

As a result of research on PDT field, there have been created some Nile Blue derivatives that may have its absorption peak in the 600-700 waveband [104]. In the clinical field, commercial Nile Blue and some selected derivatives has been showed a high biological selectivity to tumoral tissues accompanied by a quickly pharmacokinetic elimination (24 hours post administration) [104, 107]. Accordingly to Foley et al. [103], some Nile Blue chalcogens analogues can also have a great photo-induced activity against yeasts and bacteria, such as *C. albicans*, *E. coli* and *E. faecalis* [64].

Certainly, the possibility to synthetize new benzo[*a*]phenoxazinium dyes derived from Nile Blue with better pharmacologic and physic-chemical properties may be a promising approach to create new APDT photosensitizers. Benzo[*a*]phenoxazinium dyes may have some characteristics that make them good photosensitizers for APDT application. They are: broad-spectrum of action; efficient absorbers of 600-700 nm light; good cell binding and cell uptake; great photo-induced activity against pathogens; and high singlet oxygen quantum yield [103].

1.3.4. Formulation of New Concepts

The list of photosensitizers for APDT use has still expanding, especially the ones focused to inactivate pathogenic fungi such as *C. albicans*. Curcumin, chlorin e6, bacteriochlorin, boron difluoride (BF₂) or Rose Bengal (RB) are some examples of new photosensitizers that have been shown effective in killing yeasts by APDT, including *C. albicans* [62].

Alternatively, the combination of photosensitizers with compounds that create pores within the fungal membrane may increase the cellular uptake and thus, may be a potent strategy for treatment of fungal infections. Saponins and polyenes, such as amphotericin B and nystatin, are compounds with pore-forming properties that may be used in conjunction with photosensitizers on this strategy [62]. For instance, Coleman et al. [108] reported that the pretreatment of *C. albicans* cells with a saponin significantly increased the influx of Rose Bengal and Chlorin e6, as well increased 2-5 log the killing effect of this photosensitizer upon illumination with low-intensity light at the correct wavelength.

Furthermore, the emerging of a third generation photosensitizers has been also studied. This new generation has the principal aim to overcome the problem of aggregation of photosensitizer in aqueous solutions, as well as improve photosensitizer delivery and inactivation kinetics [62, 109, 110]. In this strategy, photosensitizer delivery is achieved through carriers like liposomes, micelles and nanoparticles that may be also combined with specific antibodies for the target [102, 111]. Among these carriers, liposomes are the most commonly used carrier and have been proved to enhance the killing effect of many photosensitizers by APDT. They increase photosensitizer's solubility and stability, as well as facilitate the penetration into cell by means of fusion processes or disturbing the cell wall [112].

1.4. LIGHT SOURCES AND DELIVERY

1.4.1. The concept of Light Fluence and Source Irradiance

By definition, APDT requires a light source with a wavelength that matches with absorption spectrum of the photosensitizer to supply the requested energy for inducing singlet oxygen production or promoting redox reactions. Therefore, the efficiency of APDT process is directly dependent on light exposure [9].

In light based medicine and dentistry, radiant exposure is defined as fluence and is a measurement of energy (Joule) over area (usually cm^2) of the light device spot size. Other relevant concept is the light source irradiance, which is a measurement of source power (Watt) per area (usually cm^2) of light device spot size. Typically, irradiances for light sources in antifungal PDT are in the range of $10\text{-}100 \text{ mW cm}^{-2}$, with light fluence comprised between 10 and 200 J cm^{-2} [3]. The crucial point in this light dosimetry is to avoid thermal effects of light when power outputs above 100 mW cm^{-2} are needed [62].

Indeed, there is no need to use high light doses. The anti-tumoral PDT research demonstrated that at low irradiances, oxygen consuming is lowest and thus, exposure period of tissues to singlet oxygen are longest, resulting in a high therapeutic response. Other researches in the antifungal PDT have also shown that *C. albicans* cells can be significantly killed at relatively low light intensities [62].

1.4.2. Light Penetration

The light fluences applied to the biological sites decreases exponentially with the penetration into the tissues by the combination of some dispersive and absorption effects. The proportion between these two processes is dependent on tissue type and light wavelength [66].

As is known, skin is irregular, inhomogeneous and has microscopic structures like follicles, cell organelles, macromolecules and natural chromophores, so, a portion of received photons may be reflected, dispersed or absorbed until reach the target [66]. It was of general agreement that tissue penetration of light increases with the increase of light wavelength in the visible spectrum (400-700 nm) [6, 66]. Thus, light sources with wavelength in the far red can do a good penetration into the skin, as well as photosensitizers with absorption peak in this range are the most suitable to kill dermatophytes that colonizes *stratum corneum* and hair follicles [5].

1.4.3. Most Common Light Sources in PDT

In the PDT field it has been used a wide range of lamps and lasers as light sources. While lasers provides highly coherent monochromatic light, decreasing the required time to reach a given light dose, lamps has a wide range of wavelengths so, they can be used with numerous photosensitizers. At the level of clinical treatment of localized infections on the skin or oral cavity,

both lasers and lamps provide direct illumination of the injury site. However, lasers may be used to illuminate some site of more difficult access like esophagus, by means of optical fibers with diameters less than 500 μm that can be fed through existent channels in bronchoscopes and endoscopes. Table 2 shows the most widely used lamps and lasers on PDT applications [69, 113].

Table 2. Lamps and lasers more frequent used on PDT applications. Adapted from [113]

	Light Source	Irradiance (mW cm⁻²)	Wavelength (nm)	bandwidth (nm)
Lasers	Argon laser	500-1000	488-514,5	Monochrom (5-10 nm)
	Metal vapour laser	Up to 10000	UV ou visivel (depending on metal)	
	Solid state	Up to 10000	1064; 532; 355; 266	
	Semiconductor diode laser	Up to 700	600-950	Monochrom
Lamps	Tungsten filament	Up to 250	400-1100	10-100 (depending on filters used)
	Xenon arc	Up to 300	300-1200	
	Metal halide	Up to 250	Depending on the metal, lines between 250-730	
	sodium (phosphor coated)	Up to 100	590-670	10-80 (depending on filters used)
	Fluorescent	Up to 10	400-450	≈ 30
	Light-emitting Diode (LED)	Up to 150	400-1000	(5-10 nm)

2. CHAPTER II

MATERIALS AND METHODS

2.1. Benzophenoxazines Origin

The benzophenoxazines dyes used in this work were synthesized in the Department of Chemistry of University of Minho and were gently provide by Professor Maria Sameiro Torres Gonçalves.

The benzo[*a*]phenoxazinium chlorides termed *N*[5-(3-hydroxypropylamino)-10-methyl-9*H*-benzo[*a*]phenoxazin-9-ylidene]ethanaminium chloride - **FSc** [114] and *N*[5-(11-hydroxyundecylamino)-10-methyl-9*H*-benzo[*a*]phenoxazin-9-ylidene]ethanaminium chloride - **FSd** [115] were the dyes selected for this work. As shown in Figure 6 the molecular structures of these dyes are similar, but FSd dye has a longer side chain. Table 3 also shows the main photophysical properties of these dyes.

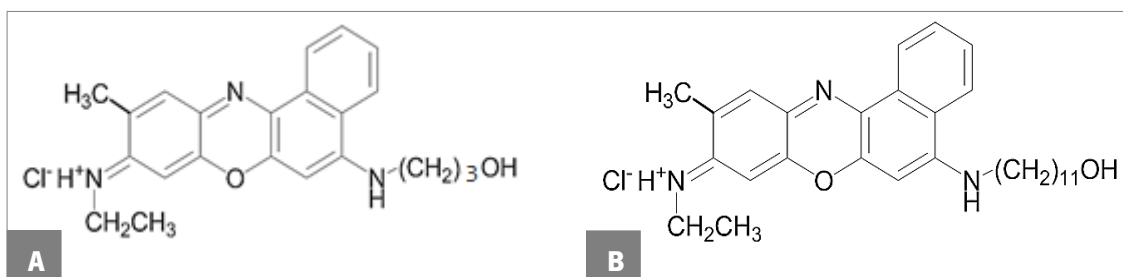


Figure 6. Chemical structure of FSc (**A**) and FSd (**B**) dyes.

Table 3. Photophysical properties of pertinent dyes.

Dye	Photophysical Properties in Ethanol				Photophysical Properties in Water (pH 7,5)			
	$\lambda_{\text{m\acute{a}x}}$ (nm) ¹	λ_{ex} (nm) ²	λ_{em} (nm) ³	Φ_{F} ⁴	$\lambda_{\text{m\acute{a}x}}$ (nm) ¹	λ_{ex} (nm) ²	λ_{em} (nm) ³	Φ_{F} ⁴
FSc	625	590	646	0.41	620	580	651	0.31
FSd	616	590	654	0.29				

¹ Wavelength of maximum absorption; ² Excitation Wavelength; ³ Emission wavelength; ⁴ Absolute fluorescence quantum yield.

2.2. Benzophenoxazines Stock Solutions

Stock solutions of each dye were prepared by solubilizing benzophenoxazines powder in Dimethyl Sulfoxide (DMSO) to a final concentration of 10 mM. Then, the solutions were transferred to 1.5 ml sterile amber microtubes (VWR Internacional, LLC. USA) to avoid ambient light and were stored at 4 °C.

Immediately before each experiment, aliquots of the dyes were diluted in sterile Phosphate Buffered Saline solution (PBS; pH 7.5; 0.1 M), which was previously prepared, to obtain working solutions with 1mM concentration. Then, these solutions were diluted again in PBS in order to obtain the required working concentrations. All the solutions were prepared on 1.5 ml sterile brown microtubes as described above.

PBS solution was prepared in sterilized water by adding 8 g l⁻¹ of sodium chloride (NaCl), 0.2 g l⁻¹ of potassium chloride (KCl), 0.3 g l⁻¹ of potassium dihydrogen phosphate (KH₂PO₄) and 1.15 g l⁻¹ of disodium phosphate (Na₂HPO₄). The pH was adjusted to 7.0 and the solution was autoclaved at 121 °C for 15 minutes and reserved at room temperature.

2.3. Organism, Culture Media and Growth Conditions

The microorganism used in this study was *Candida albicans* ATCC 90028, a reference yeast strain from American Type Culture Collection. This strain was preserved at -80°C in a storage solution of Sabouraud Dextrose Broth (SDB; Liofilchem®, Roseto degli Abruzzi, Italy) supplemented with 10% of glycerol.

SDB and Sabouraud Dextrose Agar plates (SDA; Liofilchem®, Roseto degli Abruzzi, Italy) were prepared at 30 g l⁻¹ concentration of SDB in distilled water and SDA by supplementation of SDB with 20 g l⁻¹ of agar (Liofilchem®). Then, both media were sterilized in a steam autoclave at 121°C for 15 minutes and were stored at room temperature. RPMI-1640 medium were prepared by dissolving 10.4 g l⁻¹ of this powder in distilled water and adding 34.53 g l⁻¹ of MOPS (Sigma Aldrich, Portugal). Finally the pH was adjusted to 7 and the medium was sterilized by filtration through a 0.22 µm cellulose filter.

Previously to each experiment, yeast cells were sub-cultured on SDA for 48 h at 37°C. Then, one loopful of single-cell colonies (3-5 colonies) was inoculated in 30 ml of SDB and incubated for 18 h, at 37°C, under constant agitation of 120 rpm. After this step, cells were harvested by centrifugation at 3000 x g for 10 min at 4°C and washed twice with 15 ml of PBS. The pellets were then suspended in 10 ml of sterile RPMI-1640 (Sigma Aldrich, St Louis, USA), for antifungal susceptibility testing, and in 10 ml of SDB for the remaining experiments. The cellular density was adjusted, depending on the experiment, using an improved Neubauer haemocytometer (Marienfeld, Land-Königshofen, Germany).

2.4. Antifungal Susceptibility Testing

The antifungal susceptibility testing was performed under the orientation of M27-A2 document from NCCLS - National Committee for clinical Laboratory Standards - [116] with some modifications.

Different dyes concentration at twofold final concentration (20, 25, 30, 50, 100 and 200 μM) were firstly prepared in PBS, previously to each experiment. Then, standardized cell suspensions (100 μl of containing 2×10^7 cells ml^{-1} or 2×10^8 cells ml^{-1} in RPMI) were combined with 100 μl of each dye at concentrations described above in respective wells of Biolite 96-well multidish plates (Thermo Fischer Scientific, Waltham, USA).

The microplates were incubated in the dark at 37°C during 48 h and the number of cultivable cells was then determined by counting colony forming units (CFUs). Briefly, the cell suspensions of each 3 wells per condition were collected and vortexed during 1 min. Then, serial dilutions on PBS were done and plated onto SDA. After 24 h of incubation at 37°C , the number of colonies formed was counted and the total CFUs per unit of volume were determined. These experiments were performed three times with at least each condition evaluated in triplicate. Negative, dyes and yeast controls were also included.

2.5. Biofilm Formation

Standardized cell suspensions (200 μl of containing 1×10^7 cells ml^{-1} in SDB) were placed into selected wells of 96-wells polystyrene microtiter plates (Orange Scientific, Braine-l'Alleud, Belgium) and incubated at 37°C under agitation at 120 rpm. At 24 h, 100 μl of SDB medium was removed and the same volume of fresh SDB was added. The preparations were then incubated for a further 24 h. After biofilm formation the medium was aspirated and non-adherent cells removed by washing biofilms once in 200 μl of PBS.

2.6. Quantification of Cultivable Biofilm Cells

In order to determine the number of biofilm cultivable cells on dark toxicity and photodynamic inactivation assays, the biofilms were firstly resuspended in 200 μl of PBS by scrapping the adhered biomass from the wells using a mechanic technique and repeated pipetting. Then, these 200 μl were collected to a sterile microtube and the same method was done with 100 μl of PBS to guarantee that each biofilm cell was totally resuspended. The

resulting resuspended biofilms of each 3 wells per condition (on the case of dark toxicity assay) and 2 wells per condition (on the case of photodynamic inactivation assays) were collected and vigorously vortexed during 1 min to disrupt the biofilm matrix. Then, serial decimal dilutions in PBS were done and plated onto SDA. Agar plates were incubated at 37 °C for 24 h and the total CFUs per unit area (Log CFU cm^{-2}) of microtiter plate well was enumerated.

2.7. Antifungal Photodynamic Therapy

2.7.1. Dark Toxicity

To verify the absence of antifungal activity of each dye on *C. albicans* biofilms, standardized solutions of FSc or FSd dye with 100, 200 and 300 μM concentration, previously prepared, were added to wells after biofilm formation and the microtiter plates were then incubated in the dark at 37°C during 3 h or 18 h with constant agitation at 120 rpm.

Afterwards, dye solutions were aspirated and the biofilms were washed twice in 200 μl of PBS to remove loosely attached cells and excess of dye. Then, 200 μl of PBS were added again to wells and the number of cultivable biofilm cells was determined by counting colony forming units (CFUs) as described on section 2.6. These experiments were performed three times with each condition evaluated in triplicate. Negative, dyes and yeast controls were also included.

2.7.2. Photodynamic Inactivation

In this experiment, the biofilms were formed and specific concentrations of FSc and FSd (100, 200 and 300 μM) were added (as described above) on selected wells of the microtiter plate, leaving an interval of three wells between each well used, to avoid side light exposure during biofilms illumination.

After dark incubation during 3 h or 18 h in the same conditions as described on section 2.7.1, dyes solutions were aspirated and biofilms were washed twice in 200 μl of PBS to remove loosely attached cells and excess of dye. Then, 200 μl of PBS were added again to wells and each biofilm was aseptically (assured with a Bunsen burner) illuminated at an average irradiance of 10 mW cm^{-2} with a xenon arc lamp (OSRAM HBO 200W) equipped with a bandpass filter centered on $600 \pm 2 \text{ nm}$ (ThorLabs, New Jersey, USA). Biofilms were illuminated during 20 or 60 minutes, which corresponds to a light fluence of 12 J cm^{-2} and 36 J cm^{-2} , respectively. Exact power was measured at the end of every experiment with an integrating sphere photodiode power sensor (model S144C; ThorLabs) using the PM100D Utility software (Thorlabs).

The number of cultivable biofilm cells was then determined by CFUs after biofilm cells resuspension, as described on section 2.6. Negative, dyes and yeast controls, even as light controls (illumination of biofilm with PBS only; light fluence= 12 J cm^{-2} or 36 J cm^{-2}) and dark controls (biofilm with dyes in the absence of light; light fluence= 0 J cm^{-2}) were also included. Experiments were repeated three times with each condition evaluated in duplicate.

2.7.3. Absorption Spectra of Biofilms

The absorption spectrum of each biofilm illuminated was also determined previously and after the biofilm illumination. This step was intended to observe possible dyes alterations or aggregations during light exposure. The absorption spectrum was measured using an optical fiber and the ThorLabs SPLICCO software (ThorLabs, New Jersey, USA). The selected absorption spectrum of each condition tested is on appendix A.

2.8. Dye Uptake

Dye uptake assays were realized to verify if photodynamic inactivation was correlated with dye uptake, even as to observe if that effect was influenced in a concentration-dependent manner.

After biofilm formation, biofilms were incubated in the dark with both dyes at the concentration of 100 and 300 μM during 3 h or 18 h at the same conditions as described on section 2.7.1. After dark incubation, biofilms were washed twice in 200 μl of PBS to remove excess of dye and loosely adhered cells. Then, the same volume of PBS was added and the biofilms were resuspended as described above (section 2.6). The resulting resuspended biofilms of each 3 wells per condition were collected, centrifuged at $6654 \times g$ for 5 min at 4°C and the supernatants were then collected for fluorescence analysis, to achieve dye retained in the biofilm matrix during dark incubation. These pellets were resuspended in 900 μl of PBS and cells were lysed by sonication (3 cycles of 60 seconds with 30 seconds off between each cycle, at 20 kHz and 35% of power output) through a VCX750 ultrasonic processor (Cole-Parmer, USA). The resulting lysates were centrifuged and the supernatant was removed for fluorescence analysis to achieve dye taken up by cells during dark incubation. It is important to emphasize that sonication parameters were previously optimized in order to promote the complete lysis of all biofilm cells.

For fluorescence analysis, 200 μl of each supernatant solution were placed in triplicate on selected wells of a black 96-wells pureGrade microtiter plate (VWR, Portugal). Fluorescence

was determined through a microtiter plate reader (Bio-Tek® Synergy HT, Izasa, Portugal) with excitation wavelength set to 590 nm and the emission wavelength set to 645 nm. The sensibility of device was set to 80 and the agitation intensity was defined for 1 with the duration of 3 seconds.

Results were expressed as concentration of dye on supernatant (μM). The concentration of dye was determined through previously prepared standard curves of fluorescence intensity versus concentration of dyes in PBS (Appendix B). Experiments were repeated three times with each condition evaluated in triplicate. Control wells containing biofilm with only PBS were also performed and treated as the remaining samples to determine whether PBS and the remaining biomass, even as the material plate could interfere with fluorescence intensity of the samples.

2.9. Fluorescence Microscopy

In this experiment, fluorescence microscopy analysis was performed in planktonic cells and biofilm resuspended cells, in order to observe the differences of dye uptake by cells on each approach.

2.9.1. Fluorescence Microscopy of Planktonic Cells

For fluorescence microscopy of planktonic cells, cells were inoculated in SDB for 18 h at 37°C under agitation at 120 rpm. Then, cells were harvested by centrifugation (3000 x g for 10 min at 4°C) and washed twice in 15 ml of PBS. After cells resuspension in 10 ml of PBS, the cells density was adjusted to 1×10^7 cells ml^{-1} and aliquots of 200 μl of this cell suspension was added to a 15 ml Falcon-tube (Orange Scientific, Belgium). Afterwards, these cells were harvested again by centrifugation at 1700 x g for 5 min at 4°C, resuspended in 200 μl of each dye solution at a concentration of 300 μM and incubated in the dark for 3 h or 18 h at the same conditions described on section 2.7.1. After this step, cells were harvested by centrifugation at 1700 x g for 5 min at room temperature and washed twice in 200 μl PBS. After the last wash, the resulting pellets were resuspended on 20 μl of PBS, transferred to microscope slides and examined in a BX51 Olympus Fluorescence Microscope through a TRITC filter, using the same exposure time. The obtained images are result of one single experiment with a single evaluation of each condition.

2.9.2. Fluorescence Microscopy of Biofilm Resuspended Cells

For fluorescence microscopy analysis of biofilm resuspended cells, several biofilms were formed and incubated in the dark with both dyes at the 300 μM concentration for 3 and 18 h at the same conditions described on section 2.7.1. After the dark incubation step, biofilms were washed twice in 200 μl of PBS and resuspended in the same volume of PBS through using a mechanic technique and repeated pipetting. Then, cells were harvested by centrifugation at 1700 $\times g$ for 5 min at room temperature and washed again twice in 200 μl of PBS. Then, samples were analyzed as previously described for the planktonic cells. The obtained images are result of one single experiment with a single evaluation of each condition.

2.10. Statistical Analysis

Statistical analysis was performed using the statistical program GraphPad Prism 5. All data were compared using two-way analysis of variance (ANOVA) by applying the Bonferroni post-test. Tests were performed with a confidence level of 95%.

3. CHAPTER III

RESULTS AND DISCUSSION

3.1. Antifungal Susceptibility Testing

The benzo[a]phenoxazinium chloride FSc was previously applied in planktonic *C. albicans* cells, showing potential application on APDT of this yeast species [117]. Therefore, it was important to assess the effect of this dye in *C. albicans* biofilms. Additionally, FSc was also compared with FSd dye, a new benzophenoxazinium chloride that is very similar to FSc but has a longer side chain.

Dyes were firstly compared in planktonic cells. The antifungal susceptibility testing was performed with two high cellular concentrations to mimic biofilm condition and to observe if the cellular concentration could influence the *C. albicans* susceptibility to these dyes. The viable cells were quantified by counting colony forming units (CFU). The susceptibility of both *C. albicans* cells suspensions to the benzo[a]phenoxazinium chlorides FSc and FSd is illustrated in Figure 7.

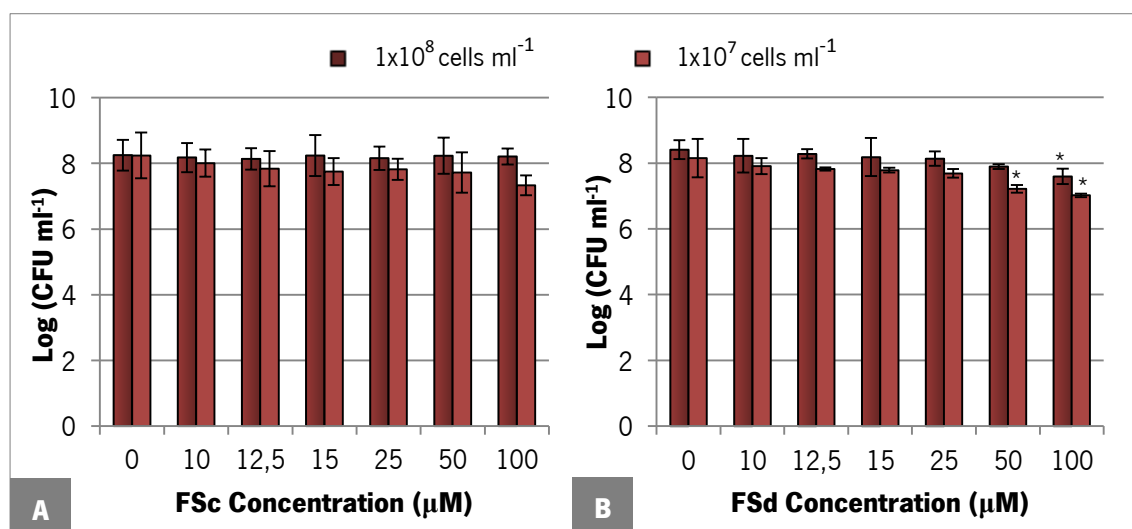


Figure 7. Susceptibility of *C. albicans* ATCC 90028 planktonic cells exposed for 48 h to FSc (**A**) and FSd (**B**) dye in RPMI. Error bars represent standard deviation. *Statistically different from the respective control, 0 μM ($P < 0.05$).

As shown in Figure 7A, for both cell concentrations used, there were no significant differences in the number of viable cells ($P > 0.05$) after treatment with different FSc concentrations and they were similar to the negative control (absence of the agent). Likewise, Figure 7B shows that the presence of FSd dye in the concentrations of 10 to 25 μM in both cell concentrations and the 50 μM concentration in the highest suspension did not cause significant changes in the number of viable cells, when compared to the respective negative control.

On the other hand, for the cell suspension of 1×10^7 cells ml^{-1} it was found significant ($P < 0.05$) growth inhibition of 0.93 log and 1.13 log when FSd concentration was 50 and 100 μM , respectively. Moreover, for the cell suspensions of 1×10^8 cells ml^{-1} there was also a small growth inhibition, but statistically significant ($P < 0.05$), of 0.81 log when the concentration of FSd was 100 μM .

In summary, the results showed on Figure 7 turns clear evident that only FSd dye can have antifungal activity against *C. albicans* suspensions in these conditions, although the growth inhibition produced by this dye was very poor. The difference on antifungal activity between these dyes may be related to their structural differences, indicating that side-chain modifications can have significant impact on their growth inhibition effect [118]. The previous work that evaluated the potential of FSc dye as a photosensitizer on *C. albicans* planktonic cells [117] also determined the susceptibility of these cells to FSc dye after 48 h. In opposition to the results presented on Figure 7, the previous susceptibility testing assays showed 90 and 100% of growth inhibition when FSc dye was used on cell suspensions of 2×10^6 cells ml^{-1} at 50 and 100 μM , respectively. The absence of the inhibitory effect observed with FSc dye in this work is perhaps related with the use of cell suspensions with higher cell density, indicating that differences on inoculum size may influence their susceptibility profile [119].

With the results obtained on the antifungal susceptibility assays it was assured that *C. albicans* suspensions with high cellular concentrations are poorly susceptible to both FSc and FSd dyes alone. The non-existent or lower antifungal activity of compounds alone is one required principle in their ideal profile as photosensitizer [5, 65]. So, these observations encouraged the transition to the APDT assays of *C. albicans* biofilms using FSc and FSd dyes as photosensitizers.

3.2. Antifungal Photodynamic Therapy

Before testing and optimizing the antifungal photodynamic efficacy of FSc and FSd dyes against *C. albicans* biofilms, dyes concentrations were firstly defined. Given that antifungal susceptibility assays showed that there is a very poor antifungal activity of dyes on concentrations tested in planktonic cells, higher concentrations of dyes (100, 200 and 300 μM) were selected for APDT assays, since usually biofilms are more resistant to antifungal drugs than their planktonic counterparts [13, 34-36].

The dark toxicity of these dyes on *C. albicans* biofilms using the set of concentrations mentioned above was firstly determined using a dark incubation period of 3 h with the intent to assess their dye alone effect using such incubation conditions. Figure 8 shows the resultant dark toxicity of both dyes on *C. albicans* biofilms.

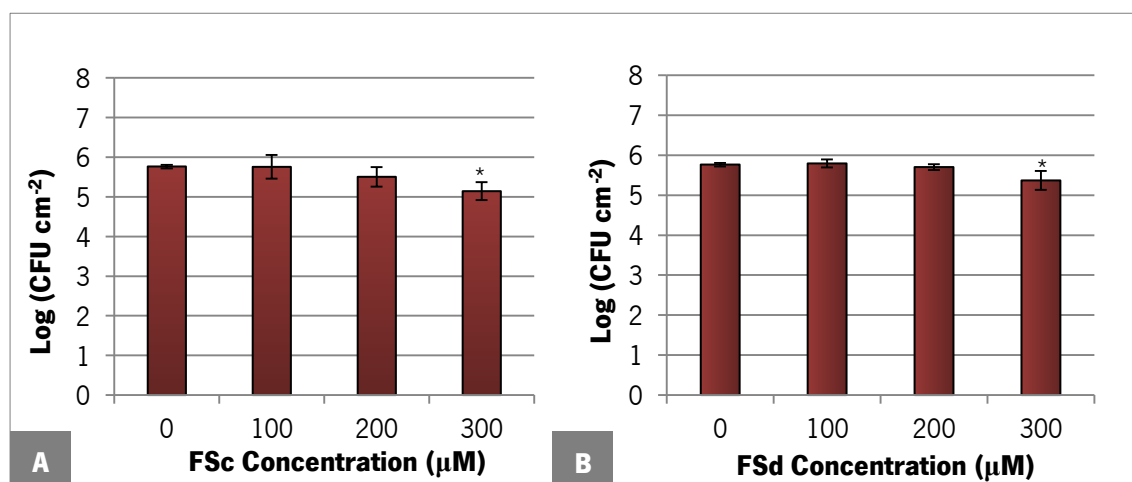


Figure 8. Logarithm of number of *C. albicans* ATCC 90028 biofilm cells per cm² after 3 h of dark incubation with FSc (A) and FSd (B) dye at different concentrations in PBS. Error bars represent standard deviation. *Statistically different from the control, 0 µM ($P < 0.05$).

As shown in Figure 8, dyes concentration of 100 and 200 µM showed no inactivation effect ($P > 0.05$) of *C. albicans* biofilms. On the other hand, it was observed a little inactivation ($P < 0.05$) of these biofilms when FSc and FSd dyes were used at 300 µM, been the killing effect at this concentration 0.62 log and 0.40 log, respectively. Indeed, it is clearly evident that dark toxicity of both dyes against *C. albicans* biofilms was very low at the conditions used. Given the clinical use of APDT ideally requires photosensitizers without dark activity, this set of dark incubation conditions could be ideal for APDT of *C. albicans* biofilms if it was achieved great levels of cell inactivation upon irradiation [5, 65]. So, such dark incubation conditions were then used in the first APDT assays of both dyes. On APDT assays, after dark incubation with dyes, biofilms were aseptically illuminated with a xenon arc lamp during 20 and 60 minutes, corresponding respectively to light fluences of 12 and 36 J cm⁻². Two controls: absence of dye only with light and absence of light, only with dye at different concentrations were also performed in parallel. The susceptibility of *C. albicans* biofilms to the photosensitization assays using FSc and FSd is shown in Figure 9.

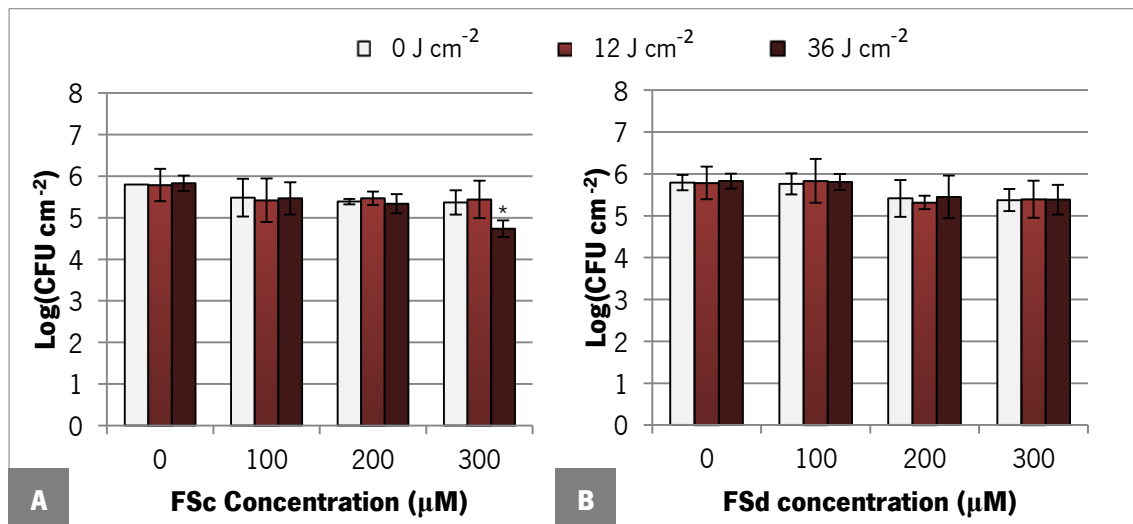


Figure 9. Logarithm of number of *C. albicans* ATCC 90028 biofilm cells per cm² after 3 h of dark incubation with FSc (A) and FSd (B) dye at different concentrations in PBS followed of exposure to various light doses. Error bars represent standard deviation. *Statistically different from the control, 0 µM ($P < 0.05$).

In comparison with the respective control of absence of light only with dyes at different concentrations (0 J cm⁻²), a statically significant ($P < 0.05$) decrease of cell viability (0.63 log) was achieved after APDT, using FSc at 300 µM and the illumination fluence of 36 J cm⁻² (60 minutes of biofilm illumination). The others APDT conditions tested with FSc and all of conditions tested with FSd dye showed no photodynamic effectiveness against *C. albicans* biofilms ($P > 0.05$). In addition, exposure to light alone had no effect on *C. albicans* cells viability.

In order to improve the photodynamic action of both dyes, it was defined a new period of contact in the dark of 18 h. This was grounded on the possible influence of dark incubation time on dye uptake that, consequently, would have an effect on APDT effectiveness of dyes [88, 120, 121]. Figure 10 presents the cell viability after 18 h of contact of biofilms with dyes.

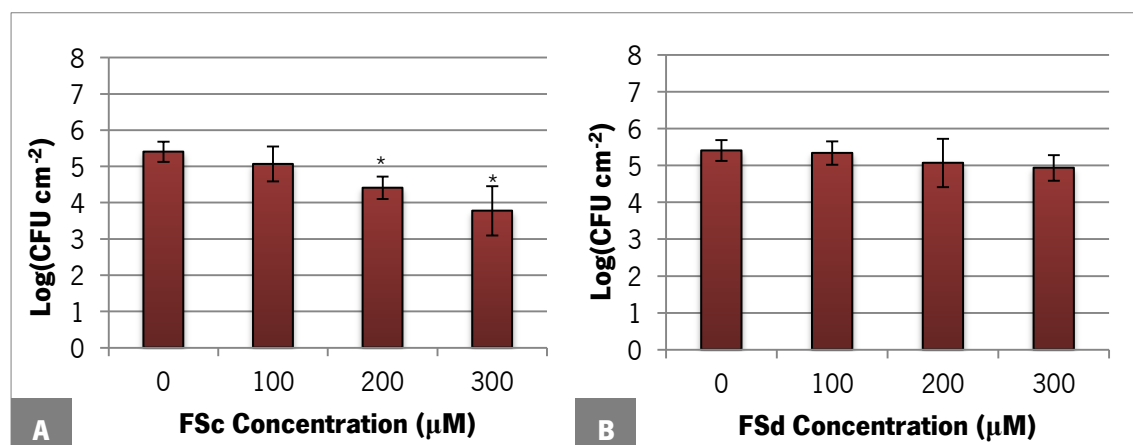


Figure 10. Logarithm of number of *C. albicans* ATCC 90028 biofilm cells per cm² after 18 h of dark incubation with both FSc and FSd dyes at different concentrations in PBS. Error bars represent standard deviation. * Statistically different from the control, 0 µM ($P < 0.05$).

Data presented in Figure 10 turns very clear that FSc dye had some dark activity in contrast to FSd dye that had no dark activity against *C. albicans* biofilms ($P>0.05$). The significant ($P<0.05$) cell viability reduction achieved with FSc dye was approximately 1 log and 1.63 log when it was used concentrations of 200 and 300 μM , respectively. However, there still was a potential to achieve higher levels of cell inactivation by performing APDT of *C. albicans* biofilms using these dark incubation conditions with dyes. So, new APDT assays were performed using such dark incubation conditions. The results of these APDT assays are presented on Figure 11.

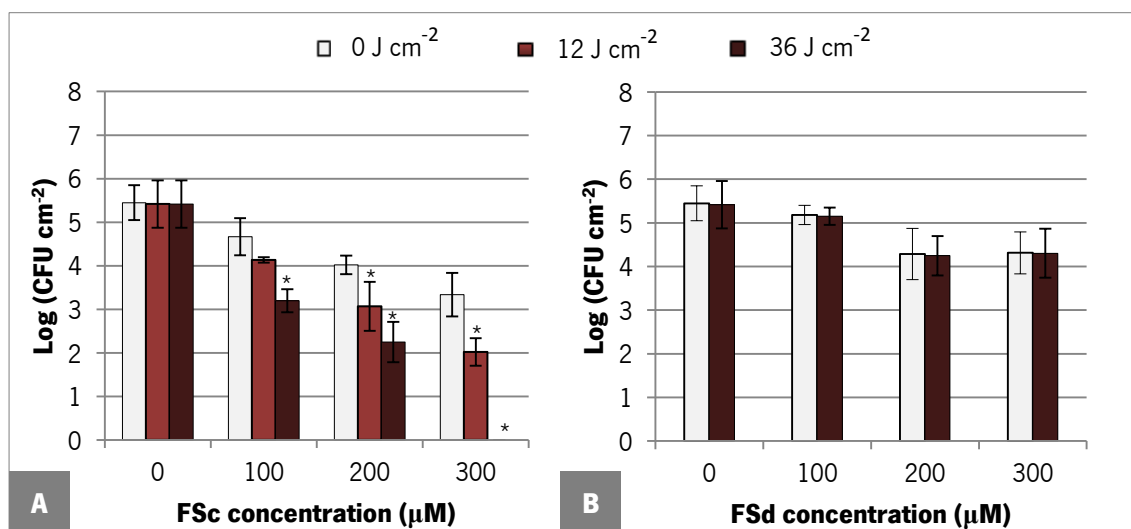


Figure 11. Logarithm of number of *C. albicans* ATCC 90028 biofilm cells per cm^2 after 18 h of dark incubation with FSc (A) and FSd (B) dye at different concentrations in PBS followed of exposure to various light doses. Error bars represent standard deviation.*Statistically different from the control, 0 μM ($P<0.05$).

The use of a longer dark incubation period turned FSc highly photodynamic effective against *C. albicans* biofilms. In comparison with the control conditions (0 J cm^{-2}), a significant decrease ($P<0.05$) of 0.95 log and 1.32 log of *C. albicans* viability was achieved when FSc concentration was, respectively, 200 μM and 300 μM , and the light fluence 12 J cm^{-2} (20 minutes of illumination). Nevertheless, the most effective conditions for photodynamic action were obtained with a light fluence of 36 J cm^{-2} (60 minutes of illumination), demonstrating that the killing effect using FSc occurs in a fluence-dependent manner [92, 98]. A significant decrease ($P<0.05$) on cell viability of 1.47 log, 1.77 log and a complete inactivation were observed when it was used FSc at 100, 200, and 300 μM , respectively, combined with a light fluence of 36 J cm^{-2} . In opposition, FSd dye showed no photodynamic action even when all dyes concentrations were combined with the highest light fluence (36 J cm^{-2}). For this reason, it was decide that the lower light fluence (12 J cm^{-2}) could be discarded of this assay.

The increasing incidence of localized fungal infections combined with the rise of drug-resistant strains has led to the investigation of new antifungal approaches. Photodynamic therapy emerged as a promising approach due to the antimicrobial effectiveness against several microorganisms. Accordingly to Kato et al. [97], APDT treatments may inhibit virulence factors and reduce *in vivo* pathogenicity of *C. albicans* without causing alterations in daughter cells, suggesting that APDT effects are transitory and strengthening that APDT approach could be indeed a promising alternative therapy to treat *C. albicans* infections. In this study it was achieved an optimal set of APDT conditions that promises a complete inactivation of *C. albicans* biofilms. With the benzo[*a*]phenoxazinium chloride termed FSc at 300 μM (119.25 mg l^{-1}) and using a dark incubation period of 18 hours followed by illumination with a light fluence of 36 J cm^{-2} , it could accomplished a complete eradication of *C. albicans* biofilms. This successfully achieve indicate that FSc-mediated APDT might be a potential new approach to treat *C. albicans* infections.

The susceptibility of fungal species to photodynamic action of several photosensitizing dyes and lights with appropriate wavelengths has been receiving increased attention in the last few years. Indeed, a complete eradication of *C. albicans* biofilms was previously reported by Teichert et al. [101] using a murine model. Nevertheless, the authors described the use a higher dye concentration (450 and 500 mg l^{-1} of MB) and higher light doses (275 J cm^{-2}). The use of similar APDT conditions to this study that inactivates *C. albicans* biofilms was reported by Dovigo et al. [87]. The study was developed using a commercial porphyrin termed Photogem® at 25 mg l^{-1} and a blue LED light at 37.5 J cm^{-2} . However, the cell viability reduction achieved was less than 1 log. In 2006, Foley et al. [103] had described so far the first benzo[*a*]phenoxazinium analogue that was highly effective in APDT of *C. albicans* – a benzo[*a*]phenoselenazinium dye. The authors achieved a 99% of cell killing when planktonic cultures of $10^7 \text{ cells ml}^{-1}$ were incubated during 10 minutes with this dye at $20 \mu\text{M}$ and then exposed to a light with only a 4 J cm^{-2} of fluence. A comparative study between FSc and the benzo[*a*]phenoselenazinium dye in the APDT of *C. albicans* biofilms, could be an interesting and enriching contribute for the research in this field.

The previous work performed with FSc dye [117] achieved a 67.1% of cell inactivation when *C. albicans* planktonic cultures of $4 \times 10^7 \text{ cells ml}^{-1}$ were incubated during 60 minutes with the FSc dye at $200 \mu\text{M}$ and illuminated at 12 J cm^{-2} of fluence. In this study it was necessary a

higher dye concentration, a longer incubation time and a higher illumination fluence to achieve a significant reduction of cell viability on *C. albicans* biofilms using FSc as photosensitizing agent. These differences on APDT conditions are due to the structural differences between planktonic and biofilm grown-cells [33]. At this respect Donnelly et al. [122] reported an interesting study. The authors designed a mucoadhesive patch containing 50 or 100 mg cm⁻² of TBO with suitable properties to be used as controlled delivery system in APDT of oropharyngeal candidosis. As a conclusion of their study, they achieved that short time period of mucoadhesive patches with this dye could be used to treat recently acquired oropharyngeal candidosis caused by planktonic cells, but longer application times of the patch or longer illumination periods may be required to treat infections caused by *C. albicans* biofilms [122]. These observations lend support to the notion that higher application times of the photosensitizer or/and longer light illumination periods are needed when biofilms are implicated.

The susceptibility of *C. albicans* biofilms to APDT by using a benzo[*a*]phenoxazinium chloride, as photosensitizing agent, is an important step in the potential use of this novel therapeutic strategy to treat fungal infections. Obviously, the issue of selectivity will be an important one, since healthy human tissues can be susceptible to damage of APDT treatments. Nevertheless, the potential for topical application of dyes and light application only to affected sites in mucocutaneous candidosis makes these infections particularly amenable to APDT [92]. Zeina et al. [123, 124] have demonstrated that APDT with MB under conditions that lead to effective killing of common skin microorganisms, including *C. albicans*, cause neither cytotoxicity nor DNA damage to keratinocytes in vitro, supporting the belief that selectivity for the microorganism may be possible for mucocutaneous candidosis. However, some in vivo data will always be important.

3.3. Dye Uptake

According to Foley et al. [103], the APDT effectiveness might depends on photochemical efficiencies of dyes, the degree of dye absorption and cell-dye binding, or both. It is interesting to note that the crossing of all APDT results using FSc suggests that increasing dye's concentration and the time of dark incubation resulted on a higher photodynamic efficacy of the dye. On the other hand, the APDT results using FSd showed that increasing dye's concentration or the

incubation period had no influence on its APDT effectiveness. In fact, the uptake of photosensitizers is an important feature for the efficacy of photoinactivation [125]. So, to demonstrate if differences on APDT effectiveness were mostly related with dye uptake, even as to observe if that effect was influenced in a concentration-dependent manner, it was accessed the concentration of dye (on the supernatant) that were retained on biofilm matrix and absorbed by *C. albicans* cells after incubation in the dark (Table 4).

Table 4. Uptake of FSc and FSd by biofilms of *C. albicans* ATCC 90028 after dark incubation with both dyes at 100 and 300 μ M in PBS for 3 h or 18 h. The values are means \pm Standard deviations

	Initial concentration of dye(μ M)	Concentration of dye on supernatant (μ M)			
		Dye retained on biofilm matrix		Dye absorbed by cells	
		3 h	18 h	3 h	18 h
F S c	100	0,54 \pm 0,03	0,89 \pm 0,25	1,49 \pm 0,43	3,46 \pm 0,44 ^{* Δ}
	300	2,22 \pm 0,21 ^{Δ}	8,69 \pm 1,03 ^{* Δ}	3,98 \pm 0,54 ^{Δ}	13,52 \pm 4,90 ^{* Δ}
F S d	100	0,48 \pm 0,31	1,25 \pm 0,21	0,13 \pm 0,02	0,70 \pm 0,04
	300	0,61 \pm 0,27	1,61 \pm 0,04	0,14 \pm 0,03	0,64 \pm 0,19

* Statistically different from the same situation at 3 h of dark incubation ($P < 0.05$).

Δ Statistically different from FSd in the same conditions ($P < 0.05$).

The results presented on table 4 confirmed that FSc dye is generally highly absorbed by biofilm matrix and *C. albicans* cells, when compared to FSd dye. Comparing both dyes in the same incubation conditions, FSc was more absorbed ($P < 0.05$) by cells when 100 μ M of the dyes were used during 18 hours in the dark. When higher concentration (300 μ M) was used, FSc was also significantly more absorbed ($P < 0.05$) by both biofilm matrix and *C. albicans* cells on all dark incubation periods used.

Interestingly, the same results (Table 4) also show that FSc uptake by the biofilm matrix and cells occurs in a concentration-dependent manner on both dark incubation periods ($P < 0.05$). Combining these remarks with the results presented in figures 10 and 13, it is clear evident the photoinactivation of *C. albicans* biofilms with this dye is significantly influenced by the dye uptake phenomenon and also its APDT outcomes were dependent on dye concentration [92, 101]. In contrast, besides the FSd uptake seems to be very poor it was not also influenced by increasing

the initial concentration of dye ($P>0.05$). Indeed, the concentration can be an important feature on dye uptake, on its cellular localization and, consequently in the photodynamic inactivation of cells [66]. The occurrence of a concentration-dependent photoinactivation of *C. albicans* was also observed previously by others authors. For instance, Bliss et al. [92] and Teichert et al. [101] reported that *C. albicans* photoinactivation using, respectively, photophrin and MB as a photosensitizing dye occurs also in a concentration-dependent manner.

The incubation time is a variable that also may affects the uptake of the dye and its cellular localization and, consequently, affects inactivation of the yeasts [66]. The results of this study showed the effectiveness of APDT on *C. albicans* biofilms using FSc is dependent on incubation time, been its best APDT outcomes achieved with the maximum period of dark incubation tested (18 hours). Comparing the results achieved on both dark incubations periods used, it was observed that there was a significant increase of dye absorbed by cells by increasing dark incubation period from 3 to 18 hours, using FSc at 100 μ M. Likewise, increasing dark incubation periods from 3 to 18 hours using an initial FSc concentration of 300 μ M resulted on a significant increase ($P<0.05$) not only of dye taken up by *C. albicans* cells but also dye retained on the biofilm matrix. In contrast, the FSd uptake was not also influenced by the incubation time ($P>0.05$). Accordingly, Jackson et al. [120], as well as Wilson and Mia [121] described that APDT of planktonic cultures of *C. albicans* using TBO was dependent on incubation time used. Moreover, Dovigo et al. [88] reported also that inactivating *C. albicans* biofilms with curcumin-mediated APDT is markedly increased with the increasing of incubation time.

In short, crossing APDT and dye uptake results emphasizes that under conditions where FSc was effectively taken up by both biofilm matrix and *C. albicans* cells, the illuminated biofilms are significantly inactivated, being the concentration of dye and the incubation time two important variables for the efficient dye uptake occurs. However, the same remarks were not observed when FSd dye is used. Therefore, the differences on APDT efficacy of FSc and FSd are perhaps mostly related with dye uptake, and so the optimal APDT outcome achieved with FSc dye is probably due to higher levels of dye uptake by the biofilm matrix and cells at the incubations conditions used. As high is the amount of dye retained on the biofilm matrix or taken up by cells, the higher will be probability to form a great amount of singlet oxygen and ROS during the light excitation, resulting on a bigger oxidative stress that leads to a better killing effect [5, 64, 65]. It is also important to denote that although the amount of dye bonded and absorbed by cells had a

crucial role to inactivate the biofilm population, dye retained on the biofilm matrix was also a crucial feature for the photodynamic inactivation of biofilms. The resulting singlet oxygen produced at this sites during illumination could exerts effect on matrix polysaccharides, leading to the biofilm destruction, or could damage the outer structures of the cell, directly allowing more dye to enter into the cell and cause cell death, accelerating the APDT effect [3, 9].

Fluorescence microscopy analysis of planktonic cells and biofilm resuspended cells after incubation in the dark during 3 and 18 h with both dyes at 300 μ M in PBS was also performed with the intent to obtain a visual result of some data presented on Table 4. Figures 12 and 13 show the resulting micrographs for planktonic cells and biofilms resuspended cells, respectively.

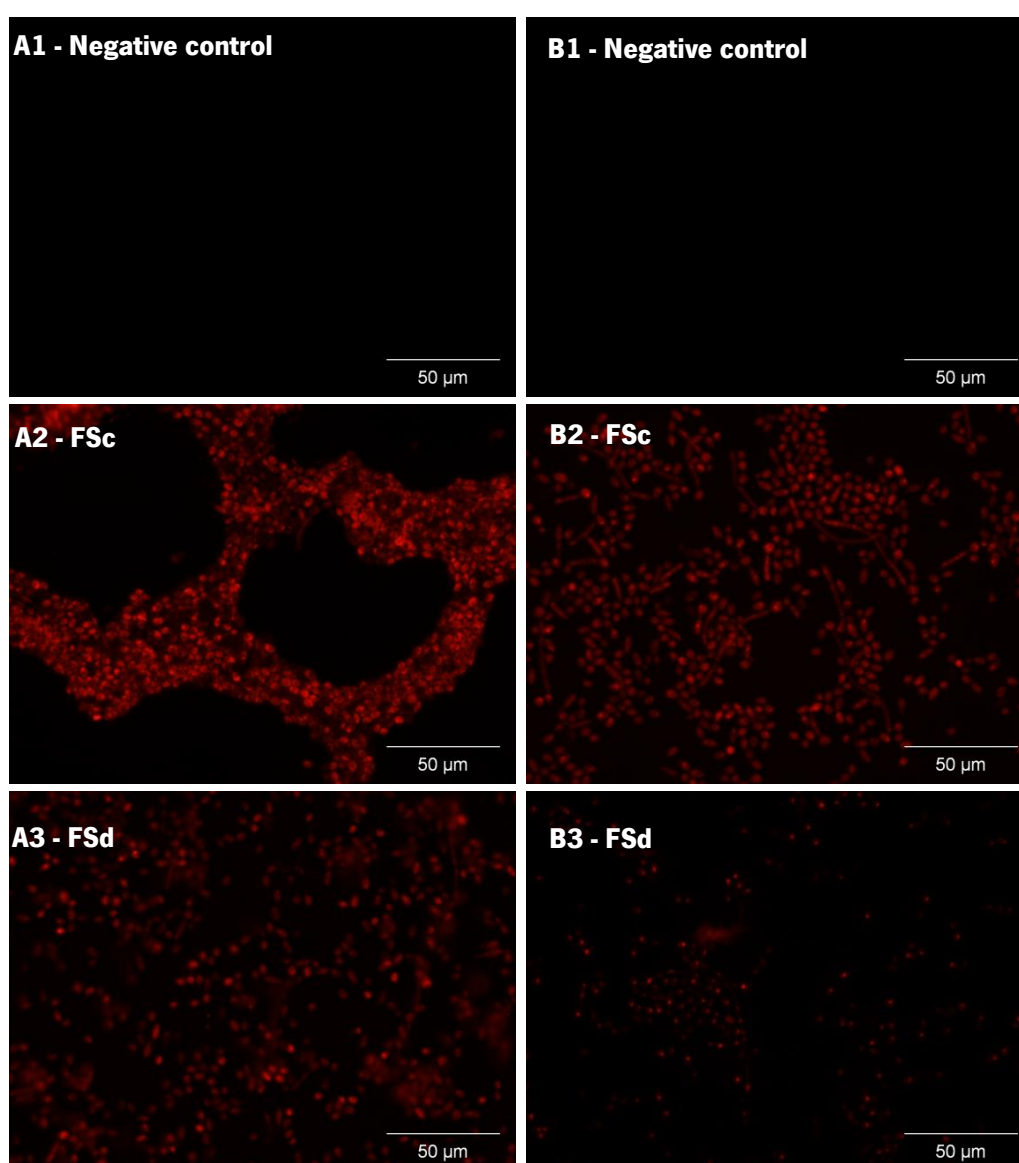


Figure 12. Fluorescence microscopy micrographs obtained for *C. albicans* ATCC 90028 planktonic cells after 3 h of incubation (**A1-A3**) and 18 h of incubation (**B1-B3**) with PBS only, as well as with FSc and FSd dye at 300 μ M in PBS.

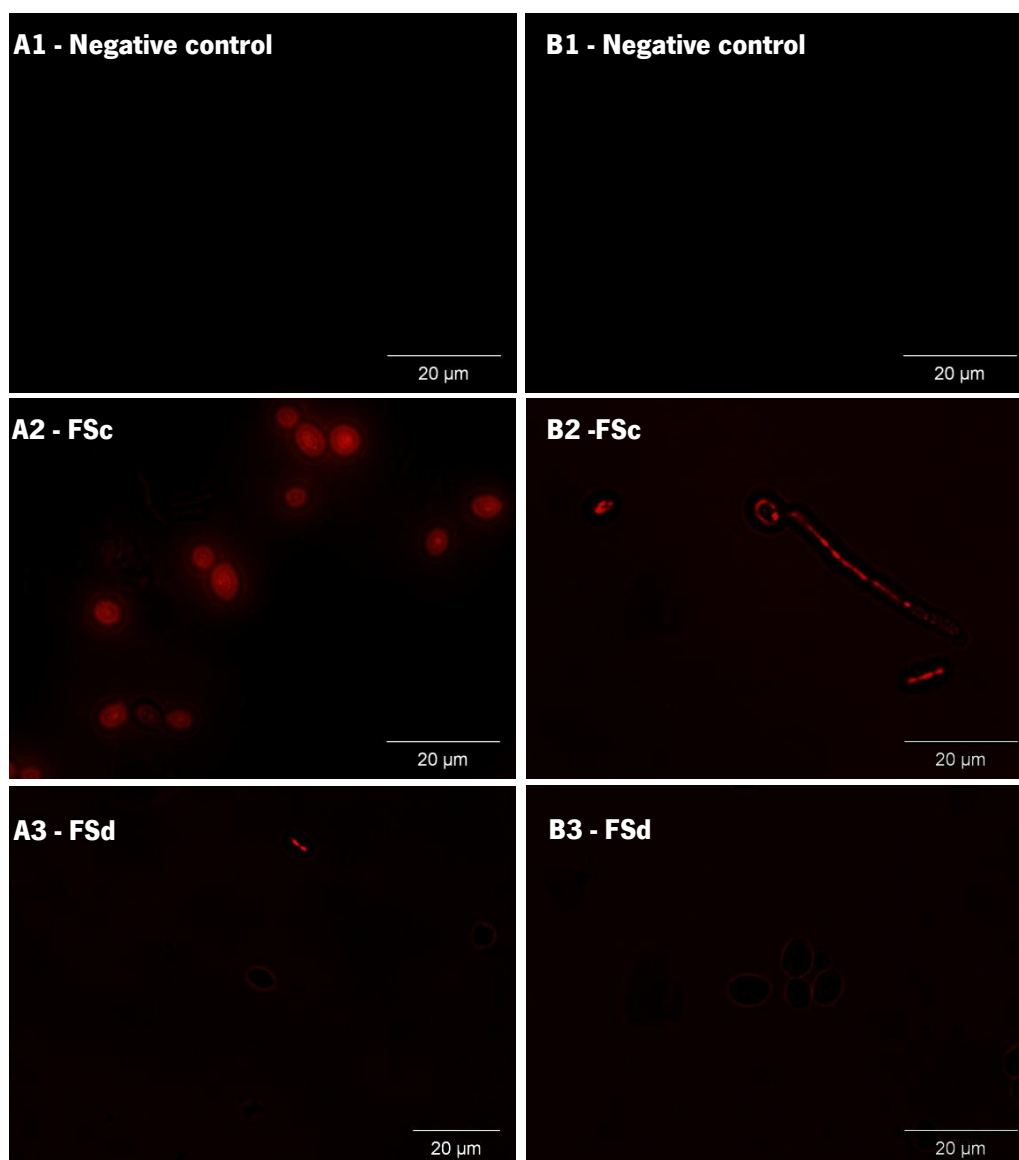


Figure 13. Fluorescence microscopy micrographs obtained for *C. albicans* ATCC 90028 biofilm resuspended cells after 3 h of dark incubation (**A1-A3**) and 18 h of dark incubation (**B1-B3**) with PBS only, as well as with FSc and FSd dye at 300 μ M in PBS.

It was possible to observe that on both situations, particularly on biofilm resuspended cells, the dark incubation with FSc resulted on higher levels of cell fluorescence, suggesting the levels of uptake of FSc was much higher than FSd dye. This qualitative analysis is in accordance with the results presented on Table 4. However, it is important to highlight that FSc and FSd have different absolute fluorescence quantum yields (Table 3), which are likely to result in some differences of fluorescence intensity observed.

Interestingly, it is also well clear on both figures that increasing the dark incubation period do not resulted on higher levels of fluorescence, as it was expected. Instead, it seems to influence the formation of little points of fluorescence, suggesting dye concentration at some cell

clusters. However, further investigations are required to confirm this observation. In fact, as it was mentioned previously, dyes can cross over the plasma membrane, especially after prolonged incubation periods, and take different subcellular localizations, such as mitochondria, nucleus, vacuoles or Golgi apparatus, as well as in endoplasmic reticulum [66]. Upon illumination, the ROS produced at these sites can cause damage to these constituents, inactivating some proteins and enzymes, oxidizing nucleic acids and peroxidizing lipids of the surface membrane, leading to the loss of cell viability [9, 72].

The higher cell fluorescence when FSd was incubated with planktonic cells, instead biofilms, was also remarkable. Figure 16 shows when there is no presence of biofilm matrix, FSd dye can do a larger binding to *C. albicans* cells, indicating that much of the small amount of dye absorbed by biofilms stays perhaps retained in the biofilm matrix.

Treatment efficacy could depend on the specificity of the compound to the target. Typically, specificity to targets could be increased by using macromolecular conjugates [118]. In this study, it was explored the possibility to enhance specificity of benzo[*a*]phenoxazinium salts to *C. albicans* cells, through small functional groups modifications. The presence of the distinct side chains on FSc and FSd dyes are presumably the responsible for distinct levels of dye uptake by *C. albicans* and, consequently, for the differences on its APDT outcomes. Besides side chain modifications may have a little effect on photophysical properties of photosensitizers [118], the presence of a longer side chain on FSd dye are presumably make more difficult its entry and diffusion throughout the biofilm matrix, impairing the cell-dye binding and dye uptake. Plus, data presented on Appendix A showed that the absorption peak of FSd dye seems to be shifted 40-70 nm to the left, in relation to the initial absorption peak (616 nm), after incubation with *C. albicans* biofilms. This shift is probably related with the formation of aggregates that absorb light at fewer wavelengths than the wavelength of maximum absorption of the dye [115, 126, 127]. The formation of dye aggregates is presumably enhancing the barrier effect of the biofilm matrix, making difficult its penetration in this structure and its arrival to cells, leading to a non-existent APDT action. Nevertheless, the hypothesis that the presence of a longer side chain on FSd molecules grants also them a higher affinity to the biofilm matrix components is not also out of the hypothesis.

4. CHAPTER IV

CONCLUSIONS AND
FUTURE PERSPECTIVES

The interest on APDT approach to treat fungal infections has been receiving an increased attention in our society in the last few years. The increasing of fungal infections due to the augmented use of indwelling devices and the growth of immunocompromised patients, as well as the emergence of drug resistant strains are the principal reasons that triggered the interest in a more effective and localized therapeutic approach to treat these microbiological diseases. Despite the numerous APDT investigations and the rising development of new photosensitizers that are photodynamic effective against a several range of pathogens, there is still a need to investigate and explore the potential of APDT approach to treat fungal infections, especially when originated by biofilms. With the intent to fill this gap of knowledge, this project aimed to evaluate and optimize the photodynamic antifungal activity of two new benzo[*a*]phenoxazinium chlorides (FSc and FSd) against *C. albicans* biofilms.

Regarding to the antifungal susceptibility testing of dyes, FSd dye showed to have a very small dark activity against *C. albicans* planktonic cells when used at 50 and 100 μM , while FSc dye showed no dark activity on all conditions tested. In relation to the antifungal photodynamic action, only FSc dye showed a photodynamic killing effect against *C. albicans* biofilms, been achieved a complete cell inactivation using FSc dye at 300 μM in contact with *C. albicans* biofilms during 18 h, followed by light exposition ($600 \pm 2 \text{ nm}$) with a fluence of 36 J cm^{-2} . The interest on benzo[*a*]phenoxazinium chlorides as photosensitizers agents to treat *C. albicans* infections by APDT grows with these results, because FSc dye showed to have an optimal photosensitizing activity in the APDT of *C. albicans* biofilms. However, it was also important to understand the uneven APDT outcomes achieved, so another important part of this study addressed the investigation of a potential correlation between dye uptake and APDT effectiveness of dyes by spectrofluorimetric analysis and fluorescence microscopy.

As a conclusion of this second part of the study, it was possible to observe that the differences in efficacy of FSc dye over FSd and the increasing of its effectiveness with incubation time are due to a higher dye uptake by the biofilm matrix and cells.

In conclusion, this study permitted to increase and to expand the knowledge about the APDT action of benzo[*a*]phenoxazinium chlorides on *C. albicans* biofilms towards new perspectives, since their APDT action on biofilms has remained unknown.

As future work, it would be interesting to determine the exactly intracellular localization of the FSc dye after the dark incubation period, in order to understand its mechanism of action. The execution of confocal microscopy analysis of biofilms incubated for long times with FSc dye may bring some important visual information about the intracellular localization of dye taken up by cells. Additionally, to determine the molecular mechanisms that lead to cell necrosis or apoptosis would be also an advance towards the knowledge about APDT action of these benzo[a]phenoxazinium chlorides.

The use of a target delivery of photosensitizers to cells is increasing and has been shown to be very promising in the APDT field. Thus, to explore the potential integration of FSc dye into nanoparticles that may be also combined with specific antibodies for the target could be an interesting approach that should be investigated. Likewise, the synergic effects of FSc-mediated APDT with compounds that create pores within the fungal membrane and increase the cellular uptake, such as amphotericin B and nystatin, may be an interesting approach that may also be explored on further investigations in this field. Nonetheless, additional information about the possible development of cellular resistance to FSc-mediated APDT treatments as well as to the combination of APDT with the strategies mentioned above should be also considered on subsequent investigations.

Given the high clinical relevance of fungal biofilms and the potential clinical application of APDT to treat candidosis, there is a substantial need to provide a deep understanding about the implications of these treatments in humans. Thus, it would be also important to evaluate the potential cytotoxic effects on mammalian cells arising from the incubation with the benzo[a]phenoxazinium chloride FSc during 18 h, as well as from the posterior combination with the light.

In real life, almost all localized infections are caused by polymicrobial biofilms, especially when a HIV-infected patient is involved. Therefore, to evaluate the effects of FSc-mediated APDT on the viability of mixed biofilms formed by pathogenic microorganisms, such as *C. albicans*, *Staphylococcus aureus* and *Staphylococcus mutans* would be very interesting. Plus, in vivo studies will be also important for the development of this new potential APDT strategy. The development of these two approaches could help to mimic the real problem of localized infections and to understand to what extent this new therapeutic strategy could treat efficiently this type of disease.

These are some of many perspectives of investigation in the field of APDT. The interest and the necessity to turn this approach in a real solution to treat superficial infections are growing and these are the main driving forces under the research in this area.

5. REFERENCES

1. Donnelly, R.F., P.A. McCarron, and M.M. Tunney, *Antifungal photodynamic therapy*. Microbiological Research, 2008. **163**(1): p. 1-12.
2. Eggimann, P., J. Garbino, and D. Pittet, *Epidemiology of Candida species infections in critically ill non-immunosuppressed patients*. The Lancet Infectious Diseases, 2003. **3**(11): p. 685-702.
3. Pereira Gonzales, F. and T. Maisch, *Photodynamic inactivation for controlling Candida albicans infections*. Fungal Biology, 2012. **116**(1): p. 1-10.
4. Sardi, J.C.O., et al., *Candida species: current epidemiology, pathogenicity, biofilm formation, natural antifungal products and new therapeutic options*. Journal of Medical Microbiology, 2013. **62**(Pt 1): p. 10-24.
5. Calzavara-Pinton, P.G., M. Venturini, and R. Sala, *A comprehensive overview of photodynamic therapy in the treatment of superficial fungal infections of the skin*. Journal of Photochemistry and Photobiology B: Biology, 2005. **78**(1): p. 1-6.
6. Maisch, T., *Anti-microbial photodynamic therapy: useful in the future?* Lasers in Medical Science, 2007. **22**(2): p. 83-91.
7. Mima, E.G.d.O., et al., *Susceptibility of Candida albicans to photodynamic therapy in a murine model of oral candidosis*. Oral Surgery, Oral Medicine, Oral Pathology, Oral Radiology, and Endodontology, 2010. **109**(3): p. 392-401.
8. Pereira, C., et al., *Susceptibility of Candida albicans, Staphylococcus aureus , and Streptococcus mutans biofilms to photodynamic inactivation: an in vitro study*. Lasers in Medical Science, 2011. **26**(3): p. 341-348.
9. Wainwright, M. and K.B. Crossley, *Photosensitising agents—circumventing resistance and breaking down biofilms: a review*. International Biodeterioration & Biodegradation, 2004. **53**(2): p. 119-126.
10. Wilson, B.C. and M.S. Patterson, *The physics, biophysics and technology of photodynamic therapy*. Physics in Medicine and Biology, 2008. **53**(9): p. R61.
11. Calderone, R.A. and W.A. Fonzi, *Virulence factors of Candida albicans*. Trends in Microbiology, 2001. **9**(7): p. 327-335.
12. Calderone, R.A. and P.C. Braun, *Adherence and receptor relationships of Candida albicans*. Microbiological Reviews, 1991. **55**(1): p. 1-20.
13. Ramage, G., et al., *Fungal Biofilm Resistance*. International Journal of Microbiology, 2012. **2012**.

14. Jori, G., et al., *Photodynamic therapy in the treatment of microbial infections: Basic principles and perspective applications*. Lasers in Surgery and Medicine, 2006. **38**(5): p. 468-481.
15. Lewis, L.E., et al., *Stage specific assessment of Candida albicans phagocytosis by macrophages identifies cell wall composition and morphogenesis as key determinants*. PLoS Pathog, 2012. **8**(3): p. e1002578.
16. Franklin, T.J. and G.A. Snow, *Vulnerable shields—the cell walls of bacteria and fungi*, in *Biochemistry and Molecular Biology of Antimicrobial Drug Action* 2005, Springer US. p. 17-45.
17. Chaffin, W.L., et al., *Cell Wall and Secreted Proteins of Candida albicans: Identification, Function, and Expression*. Microbiology and Molecular Biology Reviews, 1998. **62**(1): p. 130-180.
18. Masuoka, J., *Surface Glycans of Candida albicans and Other Pathogenic Fungi: Physiological Roles, Clinical Uses, and Experimental Challenges*. Clin Microbiol Rev, 2004. **17**(2): p. 281-310.
19. Verstrepen, K.J. and F.M. Klis, *Flocculation, adhesion and biofilm formation in yeasts*. Mol Microbiol, 2006. **60**(1): p. 5-15.
20. Kang, S. and H. Choi, *Effect of surface hydrophobicity on the adhesion of S. cerevisiae onto modified surfaces by poly(styrene-ran-sulfonic acid) random copolymers*. Colloids Surf B Biointerfaces, 2005. **46**(2): p. 70-7.
21. Klotz, S.A., et al., *Degenerate peptide recognition by Candida albicans adhesins Als5p and Als1p*. Infect Immun, 2004. **72**(4): p. 2029-34.
22. Kumamoto, C.A., *A contact-activated kinase signals Candida albicans invasive growth and biofilm development*. Proc Natl Acad Sci U S A, 2005. **102**(15): p. 5576-81.
23. Verstrepen, K.J., et al., *Intragenic tandem repeats generate functional variability*. Nat Genet, 2005. **37**(9): p. 986-90.
24. Schaller, M., et al., *Hydrolytic enzymes as virulence factors of Candida albicans*. Mycoses, 2005. **48**(6): p. 365-377.
25. Beausejour, A., et al., *Proteolytic activation of the interleukin-1beta precursor by Candida albicans*. Infect Immun, 1998. **66**(2): p. 676-81.

26. Samaranayake, Y.H., et al., *Differential phospholipase gene expression by Candida albicans in artificial media and cultured human oral epithelium*. APMIS, 2006. **114**(12): p. 857-66.
27. Jayatilake, J.A., Y.H. Samaranayake, and L.P. Samaranayake, *An ultrastructural and a cytochemical study of candidal invasion of reconstituted human oral epithelium*. J Oral Pathol Med, 2005. **34**(4): p. 240-6.
28. Stehr, F., et al., *Expression analysis of the Candida albicans lipase gene family during experimental infections and in patient samples*. FEMS Yeast Res, 2004. **4**(4-5): p. 401-8.
29. Gacser, A., et al., *Targeted gene deletion in Candida parapsilosis demonstrates the role of secreted lipase in virulence*. J Clin Invest, 2007. **117**(10): p. 3049-58.
30. Manns, J.M., D.M. Mosser, and H.R. Buckley, *Production of a hemolytic factor by Candida albicans*. Infect Immun, 1994. **62**(11): p. 5154-6.
31. Kumamoto, C.A. and M.D. Vines, *Contributions of hyphae and hypha-co-regulated genes to Candida albicans virulence*. Cellular Microbiology, 2005. **7**(11): p. 1546-1554.
32. Douglas, L.J., *Medical importance of biofilms in Candida infections*. Rev Iberoam Micol, 2002. **19**(3): p. 139-43.
33. Chandra, J., et al., *Biofilm formation by the fungal pathogen Candida albicans: development, architecture, and drug resistance*. J Bacteriol, 2001. **183**(18): p. 5385-94.
34. Douglas, L.J., *Candida biofilms and their role in infection*. Trends in Microbiology, 2003. **11**(1): p. 30-36.
35. Donlan, R.M. and J.W. Costerton, *Biofilms: survival mechanisms of clinically relevant microorganisms*. Clin Microbiol Rev, 2002. **15**(2): p. 167-93.
36. Al-Fattani, M.A. and L.J. Douglas, *Penetration of Candida Biofilms by Antifungal Agents*. Antimicrobial Agents and Chemotherapy, 2004. **48**(9): p. 3291-3297.
37. Ramage, G., et al., *Candida biofilms: an update*. Eukaryot Cell, 2005. **4**(4): p. 633-8.
38. Niimi, M., N.A. Firth, and R.D. Cannon, *Antifungal drug resistance of oral fungi*. Odontology, 2010. **98**(1): p. 15-25.
39. Baillie, G.S. and L.J. Douglas, *Effect of Growth Rate on Resistance of Candida albicans Biofilms to Antifungal Agents*. Antimicrobial Agents and Chemotherapy, 1998. **42**(8): p. 1900-1905.

40. Cannon, R.D., et al., *Candida albicans drug resistance another way to cope with stress*. Microbiology, 2007. **153**(Pt 10): p. 3211-7.
41. Mah, T.-F.C. and G.A. O'Toole, *Mechanisms of biofilm resistance to antimicrobial agents*. Trends in Microbiology, 2001. **9**(1): p. 34-39.
42. Sanglard, D., et al., *Calcineurin A of Candida albicans: involvement in antifungal tolerance, cell morphogenesis and virulence*. Mol Microbiol, 2003. **48**(4): p. 959-76.
43. Uppuluri, P., et al., *Synergistic effect of calcineurin inhibitors and fluconazole against Candida albicans biofilms*. Antimicrob Agents Chemother, 2008. **52**(3): p. 1127-32.
44. Cowen, L.E. and S. Lindquist, *Hsp90 potentiates the rapid evolution of new traits: drug resistance in diverse fungi*. Science, 2005. **309**(5744): p. 2185-9.
45. Mukherjee, P.K., et al., *Mechanism of fluconazole resistance in Candida albicans biofilms: phase-specific role of efflux pumps and membrane sterols*. Infect Immun, 2003. **71**(8): p. 4333-40.
46. Hornby, J.M., et al., *Quorum sensing in the dimorphic fungus Candida albicans is mediated by farnesol*. Appl Environ Microbiol, 2001. **67**(7): p. 2982-92.
47. Ramage, G., et al., *Investigation of multidrug efflux pumps in relation to fluconazole resistance in Candida albicans biofilms*. J Antimicrob Chemother, 2002. **49**(6): p. 973-80.
48. Ramage, G., et al., *Our current understanding of fungal biofilms*. Crit Rev Microbiol, 2009. **35**(4): p. 340-55.
49. Nett, J.E., et al., *Genetic basis of Candida biofilm resistance due to drug-sequestering matrix glucan*. J Infect Dis, 2010. **202**(1): p. 171-5.
50. Nobile, C.J., et al., *Biofilm matrix regulation by Candida albicans Zap1*. PLoS Biol, 2009. **7**(6): p. e1000133.
51. Anderson, J.B., *Evolution of antifungal-drug resistance: mechanisms and pathogen fitness*. Nat Rev Microbiol, 2005. **3**(7): p. 547-56.
52. García-Sánchez, S., et al., *Candida albicans Biofilms: a Developmental State Associated With Specific and Stable Gene Expression Patterns*. Eukaryotic Cell, 2004. **3**(2): p. 536-545.
53. Albertson, G.D., et al., *Multiple efflux mechanisms are involved in Candida albicans fluconazole resistance*. Antimicrob Agents Chemother, 1996. **40**(12): p. 2835-41.

54. Piddock, L.J., *Multidrug-resistance efflux pumps - not just for resistance*. Nat Rev Microbiol, 2006. **4**(8): p. 629-36.
55. Akins, R.A., *An update on antifungal targets and mechanisms of resistance in Candida albicans*. Med Mycol, 2005. **43**(4): p. 285-318.
56. Wang, H., et al., *Rapid detection of ERG11 gene mutations in clinical Candida albicans isolates with reduced susceptibility to fluconazole by rolling circle amplification and DNA sequencing*. BMC Microbiol, 2009. **9**: p. 167.
57. Lewis, K., *Riddle of Biofilm Resistance*. Antimicrobial Agents and Chemotherapy, 2001. **45**(4): p. 999-1007.
58. Lewis, K., *Persister cells*. Annu Rev Microbiol, 2010. **64**: p. 357-72.
59. LaFleur, M.D., C.A. Kumamoto, and K. Lewis, *Candida albicans Biofilms Produce Antifungal-Tolerant Persister Cells*. Antimicrobial Agents and Chemotherapy, 2006. **50**(11): p. 3839-3846.
60. Zhu, T.C. and J.C. Finlay, *The role of photodynamic therapy (PDT) physics*. Med Phys, 2008. **35**(7): p. 3127-36.
61. Lee, Y. and E.D. Baron, *Photodynamic Therapy: Current Evidence and Applications in Dermatology*. Seminars in Cutaneous Medicine and Surgery, 2011. **30**(4): p. 199-209.
62. Dai, T., et al., *Concepts and principles of photodynamic therapy as an alternative antifungal discovery platform*. Front Microbiol, 2012. **3**: p. 120.
63. St. Denis, T.G., et al., *Analysis of the Bacterial Heat Shock Response to Photodynamic Therapy-mediated Oxidative Stress*. Photochemistry and Photobiology, 2011. **87**(3): p. 707-713.
64. Yano, S., et al., *Current states and future views in photodynamic therapy*. Journal of Photochemistry and Photobiology C: Photochemistry Reviews, 2011. **12**(1): p. 46-67.
65. Nyman, E.S. and P.H. Hynninen, *Research advances in the use of tetrapyrrolic photosensitizers for photodynamic therapy*. Journal of Photochemistry and Photobiology B: Biology, 2004. **73**(1-2): p. 1-28.
66. Castano, A.P., T.N. Demidova, and M.R. Hamblin, *Mechanisms in photodynamic therapy: part one—photosensitizers, photochemistry and cellular localization*. Photodiagnosis and Photodynamic Therapy, 2004. **1**(4): p. 279-293.

67. Ochsner, M., *Photophysical and photobiological processes in the photodynamic therapy of tumours*. Journal of Photochemistry and Photobiology B: Biology, 1997. **39**(1): p. 1-18.
68. Valko, M., H. Morris, and M.T.D. Cronin, *Metals, Toxicity and Oxidative Stress*. Current Medicinal Chemistry, 2005. **12**(10): p. 1161-1208.
69. Macdonald, I.J. and T.J. Dougherty, *Basic principles of photodynamic therapy*. Journal of Porphyrins and Phthalocyanines, 2001. **5**(2): p. 105-129.
70. Plaetzer, K., et al., *Photophysics and photochemistry of photodynamic therapy: fundamental aspects*. Lasers in Medical Science, 2009. **24**(2): p. 259-268.
71. Robertson, C.A., D.H. Evans, and H. Abrahamse, *Photodynamic therapy (PDT): A short review on cellular mechanisms and cancer research applications for PDT*. Journal of Photochemistry and Photobiology B: Biology, 2009. **96**(1): p. 1-8.
72. Paardekooper, M., et al., *Intracellular Damage In Yeast Cells Caused By Photodynamic Treatment With Toluidine Blue*. Photochemistry and Photobiology, 1995. **61**(1): p. 84-89.
73. Amaral, L., et al., *Phenothiazines, Bacterial Efflux Pumps and Targeting the Macrophage for Enhanced Killing of Intracellular XDR TB*. In Vivo, 2010. **24**(4): p. 409-424.
74. Bertoloni, G., et al., *Photosensitizing activity of hematoporphyrin on Staphylococcus aureus cells*. Biochimica et Biophysica Acta (BBA) - General Subjects, 2000. **1475**(2): p. 169-174.
75. Lambrechts, S.A.G., M.C.G. Aalders, and J. Van Marle, *Mechanistic Study of the Photodynamic Inactivation of Candida albicans by a Cationic Porphyrin*. Antimicrobial Agents and Chemotherapy, 2005. **49**(5): p. 2026-2034.
76. Valduga, G., et al., *Photosensitization of Wild and Mutant Strains of Escherichia coli by meso-Tetra (N-methyl-4-pyridyl)porphine*. Biochemical and Biophysical Research Communications, 1999. **256**(1): p. 84-88.
77. Kishen, A., et al., *Efflux Pump Inhibitor Potentiates Antimicrobial Photodynamic Inactivation of Enterococcus faecalis Biofilm*. Photochemistry and Photobiology, 2010. **86**(6): p. 1343-1349.
78. Collins, T., et al., *The Effect of a Cationic Porphyrin on Pseudomonas aeruginosa Biofilms*. Current Microbiology, 2010. **61**(5): p. 411-416.

79. Casas, A., et al., *Mechanisms of Resistance to Photodynamic Therapy*. Current Medicinal Chemistry, 2011. **18**(16): p. 2486-2515.
80. Price, M., S.R. Terlecky, and D. Kessel, *A role for hydrogen peroxide in the pro-apoptotic effects of photodynamic therapy*. Photochem Photobiol, 2009. **85**(6): p. 1491-6.
81. Kim, S.Y., O.J. Kwon, and J.-W. Park, *Inactivation of catalase and superoxide dismutase by singlet oxygen derived from photoactivated dye*. Biochimie, 2001. **83**(5): p. 437-444.
82. Prates, R.A., et al., *Influence of multidrug efflux systems on methylene blue-mediated photodynamic inactivation of Candida albicans*. Journal of Antimicrobial Chemotherapy, 2011. **66**(7): p. 1525-1532.
83. Shackley, D.C., et al., *Comparison of the cellular molecular stress responses after treatments used in bladder cancer*. BJU International, 2002. **90**(9): p. 924-932.
84. Zeina, B., et al., *Killing of cutaneous microbial species by photodynamic therapy*. British Journal of Dermatology, 2001. **144**(2): p. 274-278.
85. Reddi, E., et al., *Photophysical Properties and Antibacterial Activity of Meso-substituted Cationic Porphyrins*. Photochemistry and Photobiology, 2002. **75**(5): p. 462-470.
86. Soukos, N.S., et al., *Photodynamic effects of toluidine blue on human oral keratinocytes and fibroblasts and Streptococcus sanguis evaluated in vitro*. Lasers in Surgery and Medicine, 1996. **18**(3): p. 253-259.
87. Dovigo, L.N., et al., *Fungicidal effect of photodynamic therapy against fluconazole-resistant Candida albicans and Candida glabrata*. Mycoses, 2011. **54**(2): p. 123-130.
88. Dovigo, L.N., et al., *Investigation of the Photodynamic Effects of Curcumin Against Candida albicans*. Photochemistry and Photobiology, 2011. **87**(4): p. 895-903.
89. Dovigo, L.N., et al., *Susceptibility of clinical isolates of Candida to photodynamic effects of curcumin*. Lasers in Surgery and Medicine, 2011. **43**(9): p. 927-934.
90. Chabrier-Roselló, Y., et al., *Inhibition of electron transport chain assembly and function promotes photodynamic killing of Candida*. Journal of Photochemistry and Photobiology B: Biology, 2010. **99**(3): p. 117-125.
91. Chabrier-Roselló, Y., et al., *Sensitivity of Candida albicans Germ Tubes and Biofilms to Photofrin-Mediated Phototoxicity*. Antimicrobial Agents and Chemotherapy, 2005. **49**(10): p. 4288-4295.
92. Bliss, J.M., et al., *Susceptibility of Candida Species to Photodynamic Effects of Photofrin*. Antimicrobial Agents and Chemotherapy, 2004. **48**(6): p. 2000-2006.

93. Quiroga, E.D., M.G. Alvarez, and E.N. Durantini, *Susceptibility of Candida albicans to photodynamic action of 5,10,15,20-tetra(4-N-methylpyridyl)porphyrin in different media*. FEMS Immunology & Medical Microbiology, 2010. **60**(2): p. 123-131.
94. Lam, M., et al., *Photodynamic Therapy with Pc 4 Induces Apoptosis of Candida albicans*. Photochemistry and Photobiology, 2011. **87**(4): p. 904-909.
95. Donnelly, R.F., et al., *Delivery of Methylene Blue and meso-tetra (N-methyl-4-pyridyl) porphine tetra tosylate from cross-linked poly(vinyl alcohol) hydrogels: A potential means of photodynamic therapy of infected wounds*. Journal of Photochemistry and Photobiology B: Biology, 2009. **96**(3): p. 223-231.
96. Mitra, S., et al., *Effective photosensitization and selectivity In Vivo of Candida Albicans by meso-tetra (N-methyl-4-pyridyl) porphine tetra tosylate*. Lasers in Surgery and Medicine, 2011. **43**(4): p. 324-332.
97. Kato, I.T., et al., *Antimicrobial Photodynamic Inactivation Inhibits Candida albicans Virulence Factors and Reduces In Vivo Pathogenicity*. Antimicrobial Agents and Chemotherapy, 2013. **57**(1): p. 445-451.
98. Mang, T.S., L. Mikulski, and R.E. Hall, *Photodynamic inactivation of normal and antifungal resistant Candida species*. Photodiagnosis Photodyn Ther, 2010. **7**(2): p. 98-105.
99. Soares, B.M., et al., *In vitro photodynamic inactivation of Candida spp. growth and adhesion to buccal epithelial cells*. Journal of Photochemistry and Photobiology B: Biology, 2009. **94**(1): p. 65-70.
100. Biel, M.A., et al., *Antimicrobial photodynamic therapy treatment of chronic recurrent sinusitis biofilms*. International Forum of Allergy & Rhinology, 2011. **1**(5): p. 329-334.
101. Teichert, M.C., et al., *Treatment of oral candidiasis with methylene blue-mediated photodynamic therapy in an immunodeficient murine model*. Oral Surg Oral Med Oral Pathol Oral Radiol Endod, 2002. **93**(2): p. 155-60.
102. Wöhrle, D., et al., *Photodynamic therapy of cancer: Second and third generations of photosensitizers*. Russian Chemical Bulletin, 1998. **47**(5): p. 807-816.
103. Foley, J.W., et al., *Synthesis and Properties of Benzo[a]phenoxazinium Chalcogen Analogues as Novel Broad-Spectrum Antimicrobial Photosensitizers*. Journal of Medicinal Chemistry, 2006. **49**(17): p. 5291-5299.

104. Jose, J. and K. Burgess, *Benzophenoxazine-based fluorescent dyes for labeling biomolecules*. Tetrahedron, 2006. **62**(48): p. 11021-11037.
105. Monfrecola, G., et al., *In vitro effect of 5-aminolaevulinic acid plus visible light on Candida albicans*. Photochemical & Photobiological Sciences, 2004. **3**(5): p. 419-422.
106. Oriel, S. and Y. Nitzan, *Photoinactivation of Candida albicans by Its Own Endogenous Porphyrins*. Current Microbiology, 2010. **60**(2): p. 117-123.
107. Lewis, M.R., P.P. Goland, and H.A. Sloviter, *The Action of Oxazine Dyes on Tumors in Mice*. Cancer Research, 1949. **9**(12): p. 736-740.
108. Coleman, J.J., et al., *Characterization of Plant-Derived Saponin Natural Products against Candida albicans*. ACS Chemical Biology, 2010. **5**(3): p. 321-332.
109. Mantareva, V., et al., *Photodynamic efficacy of water-soluble Si(IV) and Ge(IV) phthalocyanines towards Candida albicans planktonic and biofilm cultures*. European Journal of Medicinal Chemistry, 2011. **46**(9): p. 4430-4440.
110. Khan, S., et al., *Gold nanoparticles enhance methylene blue-induced photodynamic therapy: a novel therapeutic approach to inhibit Candida albicans biofilm*. Int J Nanomedicine, 2012. **7**: p. 3245-57.
111. Josefsen, L.B. and R.W. Boyle, *Photodynamic therapy: novel third-generation photosensitizers one step closer?* British Journal of Pharmacology, 2008. **154**(1): p. 1-3.
112. Jia, Y., H. Joly, and A. Omri, *Characterization of the interaction between liposomal formulations and Pseudomonas aeruginosa*. Journal of Liposome Research, 2010. **20**(2): p. 134-146.
113. Brancalion, L. and H. Moseley, *Laser and Non-laser Light Sources for Photodynamic Therapy*. Lasers in Medical Science, 2002. **17**(3): p. 173-186.
114. Frade, V.H.J., et al., *Functionalised benzo[a]phenoxazine dyes as long-wavelength fluorescent probes for amino acids*. Tetrahedron, 2007. **63**(7): p. 1654-1663.
115. Alves, C.M.A., et al., *Novel DNA fluorescence probes based on N-[5-(11-functionalised-undecylamino)-9H-benzo[a]phenoxazin-9-ylidene]propan-1-aminium chlorides: synthesis and photophysical studies*. Tetrahedron Letters, 2011. **52**(1): p. 112-116.
116. NCCLS, *Reference Method for Broth Dilution Antifungal Susceptibility Testing of Yeasts*. Approved Standard-Second Edition. NCCLS document M27-A2, 2002.

117. Pereira, J.P., *Aplicação de Novos Antifúngicos do Tipo Benzofenoxazinas no Controlo de Infecções: Avaliação do Potencial Uso em Fototerapia Dinâmica*, in *Biological Engineering Department* 2009, University of Minho.
118. Verma, S., et al., *Antimicrobial Photodynamic Efficacy of Side-chain Functionalized Benzo[a]phenothiazinium Dyes*. *Photochemistry and Photobiology*, 2009. **85**(1): p. 111-118.
119. Perumal, P., S. Mekala, and W.L. Chaffin, *Role for Cell Density in Antifungal Drug Resistance in Candida albicans Biofilms*. *Antimicrobial Agents and Chemotherapy*, 2007. **51**(7): p. 2454-2463.
120. Jackson, Z., et al., *Killing of the Yeast and Hyphal Forms of Candida albicans Using a Light-Activated Antimicrobial Agent*. *Lasers in Medical Science*, 1999. **14**(2): p. 150-157.
121. Wilson, M. and N. Mia, *Effect of environmental factors on the lethal photosensitization of Candida albicans in vitro*. *Lasers in Medical Science*, 1994. **9**(2): p. 105-109.
122. Donnelly, R.F., et al., *Potential of photodynamic therapy in treatment of fungal infections of the mouth. Design and characterisation of a mucoadhesive patch containing toluidine blue O*. *Journal of Photochemistry and Photobiology B: Biology*, 2007. **86**(1): p. 59-69.
123. Zeina, B., et al., *Antimicrobial photodynamic therapy: assessment of genotoxic effects on keratinocytes in vitro*. *Br J Dermatol*, 2003. **148**(2): p. 229-32.
124. Zeina, B., et al., *Cytotoxic effects of antimicrobial photodynamic therapy on keratinocytes in vitro*. *Br J Dermatol*, 2002. **146**(4): p. 568-73.
125. Zheng, B.-Y., et al., *Photodynamic inactivation of Candida albicans sensitized by a series of novel axially di-substituted silicon (IV) phthalocyanines*. *Dyes and Pigments*, 2012(0).
126. Frade, V.H.J., et al., *Synthesis and spectral properties of long-wavelength fluorescent dyes*. *Journal of Photochemistry and Photobiology A: Chemistry*, 2007. **185**(2–3): p. 220-230.
127. Rama Raju, B., et al., *Novel Nile Blue derivatives as fluorescent probes for DNA*. *Dyes and Pigments*, 2013. **99**(1): p. 220-227.
128. Guilbault, G.G., *Practical fluorescence : theory, methods, and techniques* 1973, New York: Dekker.

6. APPENDICES

Appendix A - Absorption Spectra of Biofilms

As mentioned on section 2.7.3. selected absorption spectrum of illuminated biofilms are presented below (Figures A1 to A7). The absorption spectra were determined for each condition performed on photodynamic inactivation assays previously and after light exposure.

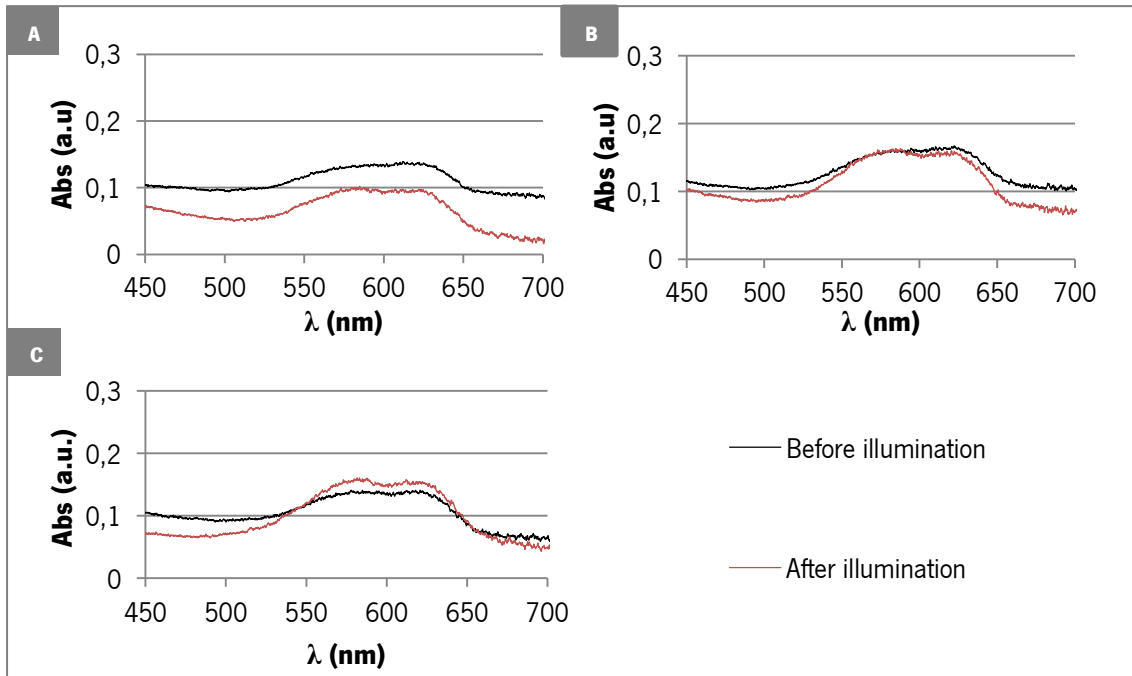


Figure A 1. Absorption spectra of biofilms of *Candida albicans* ATCC 90028 before and after exposure to a light fluence of 12 J cm^{-2} following 3 h of incubation with FSc dye at 100 μM (A), 200 μM (B) and 300 μM (C) in PBS.

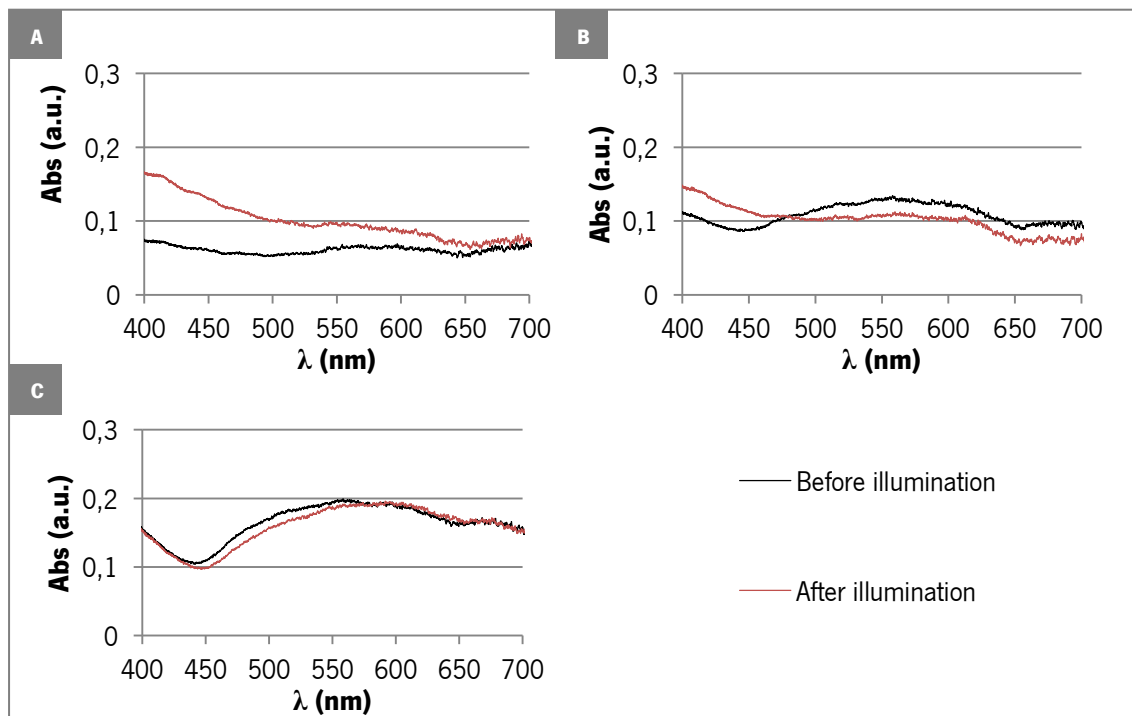


Figure A 2. Absorption spectra of biofilms of *Candida albicans* ATCC 90028 before and after exposure to a light fluence of 12 J cm^{-2} following 3 h of incubation with Fsd dye at 100 μM (A), 200 μM (B) and 300 μM (C) in PBS.

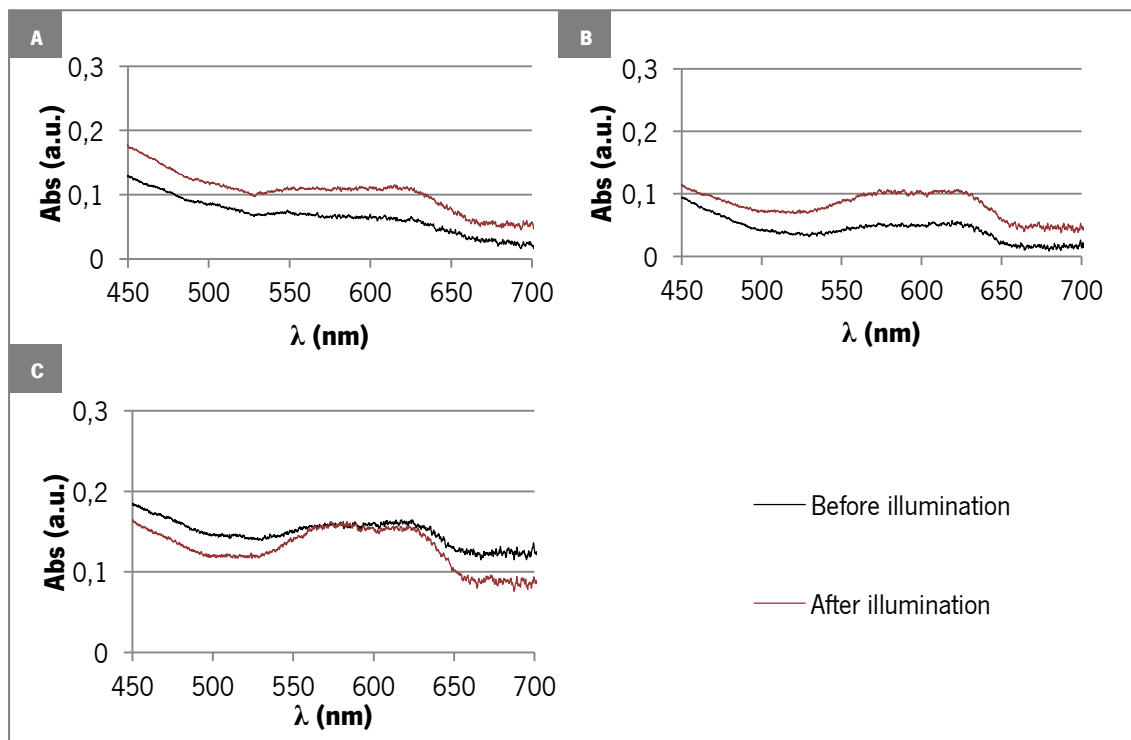


Figure A 3. Absorption spectra of biofilms of *Candida albicans* ATCC 90028 before and after exposure to a light fluence of 36 J cm^{-2} following 3 h of incubation with FSc dye at 100 μM (A), 200 μM (B) and 300 μM (C) in PBS.

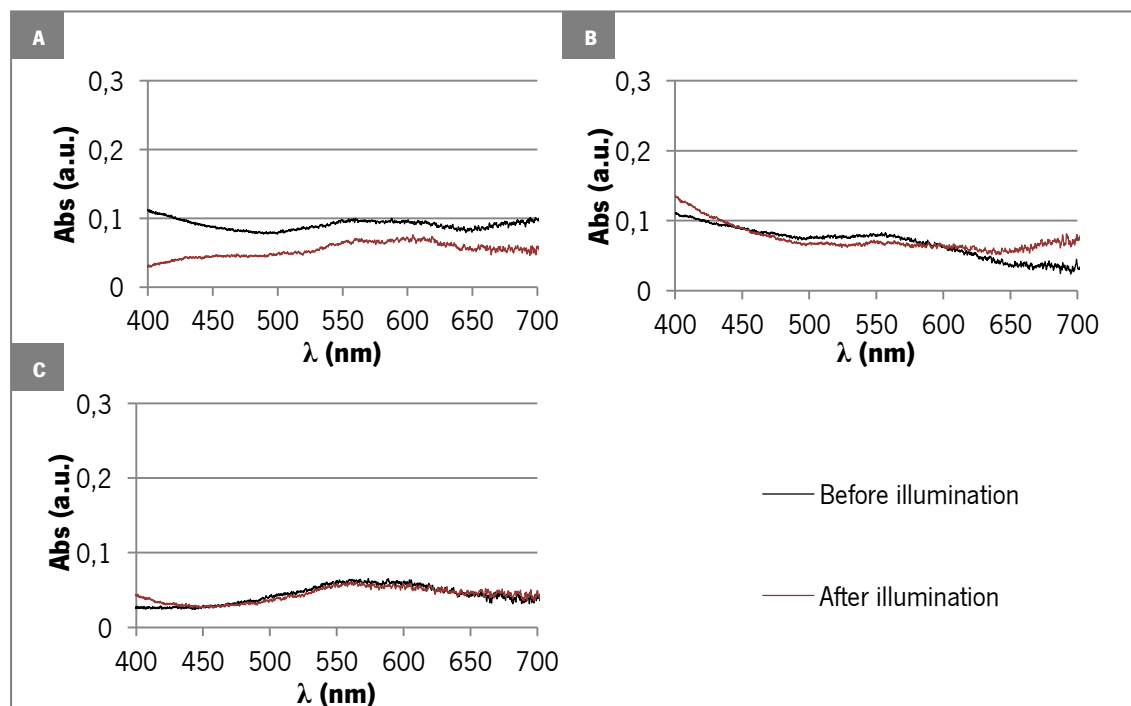


Figure A 4. Absorption spectra of biofilms of *Candida albicans* ATCC 90028 before and after exposure to a light fluence of 36 J cm^{-2} following 3 h of incubation with FSd dye at 100 μM (A), 200 μM (B) and 300 μM (C) in PBS.

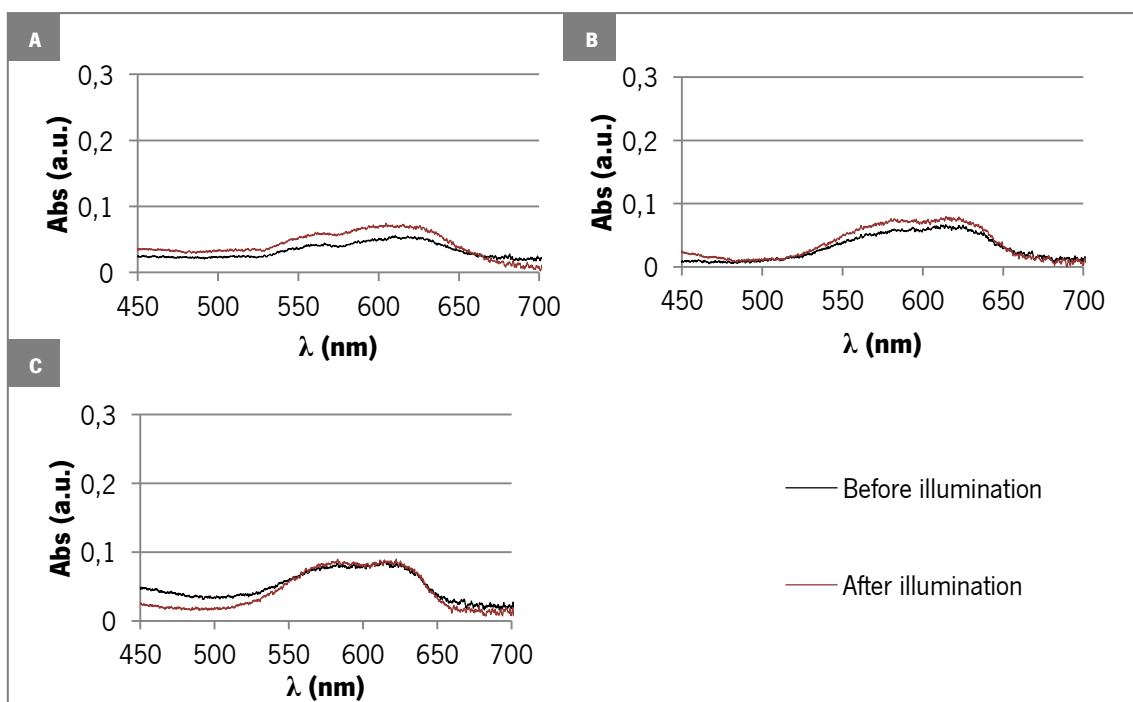


Figure A 5. Absorption spectra of biofilms of *Candida albicans* ATCC 90028 before and after exposure to a light fluence of 12 J cm^{-2} following 18 h of incubation with FSc dye at 100 μM (A), 200 μM (B) and 300 μM (C) in PBS.

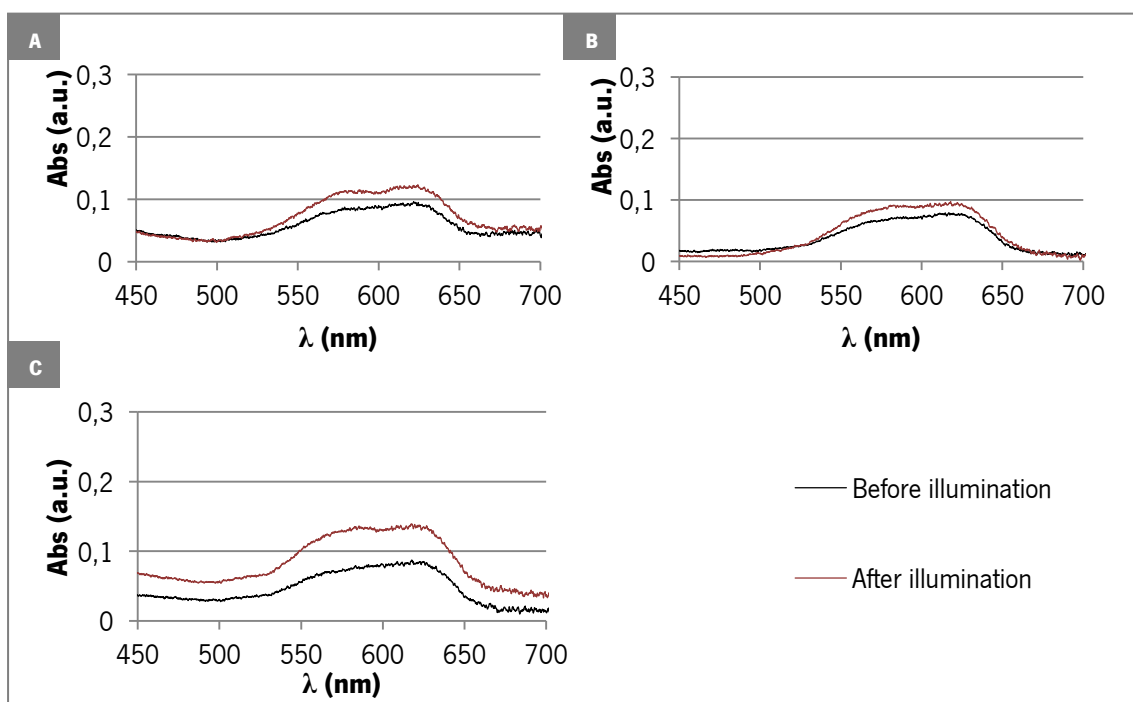


Figure A 6. Absorption spectra of biofilms of *Candida albicans* ATCC 90028 before and after exposure to a light fluence of 36 J cm^{-2} following 18 h of incubation with FSc dye at 100 μM (A), 200 μM (B) and 300 μM (C) in PBS.

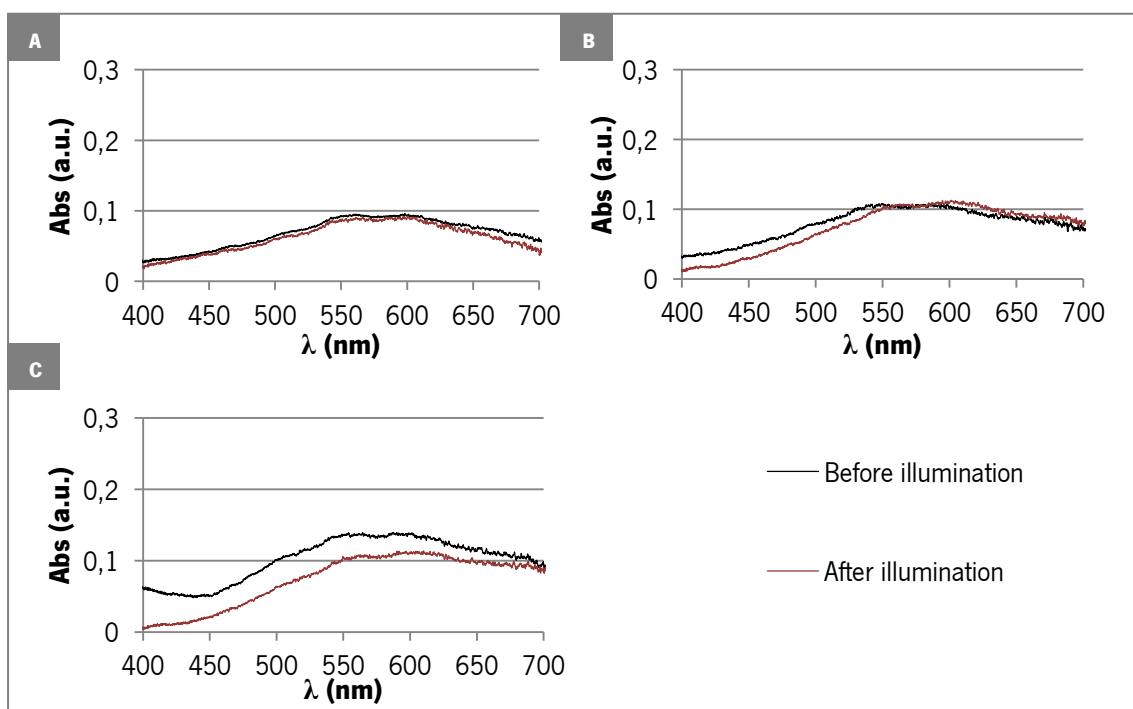


Figure A 7. Absorption spectra of biofilms of *Candida albicans* ATCC 90028 before and after exposure to a light fluence of 36 J cm^{-2} following 18 h of incubation with FSD dye at 100 μM (A), 200 μM (B) and 300 μM (C) in PBS.

Appendix B – Calibration Curves

As described by Guilbault, G. [128], calibration curves of fluorescence intensity versus concentration of dye were determined only for dyes concentrations with absorbance below 0.1 to avoid the phenomenon of concentration quenching of fluorescence, in which high concentrations of dye may result on low fluorescence intensity response. Therefore, calibration curves of absorbance versus concentration of dye in PBS were firstly determined, at the respective wavelength of maximum absorption of each dye. Figures B1 and B2 show the calibration curves of absorbance for FSc and FSd dye, respectively. Figures B3 and B4 show the respective calibration curves of fluorescence intensity for FSc and FSd that were posteriorly determined with excitation wavelength set to 590 nm and the emission wavelength set to 645 nm.

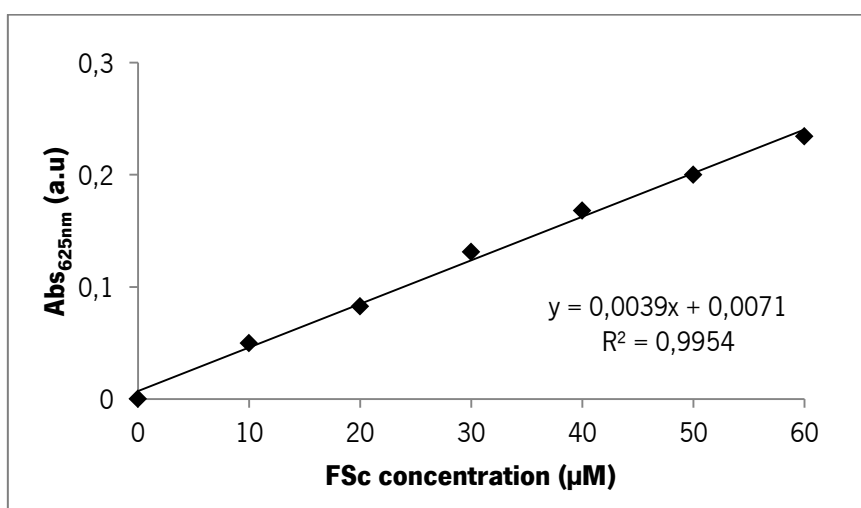


Figure B 1. Calibration curve of absorbance versus FSc dye concentration.

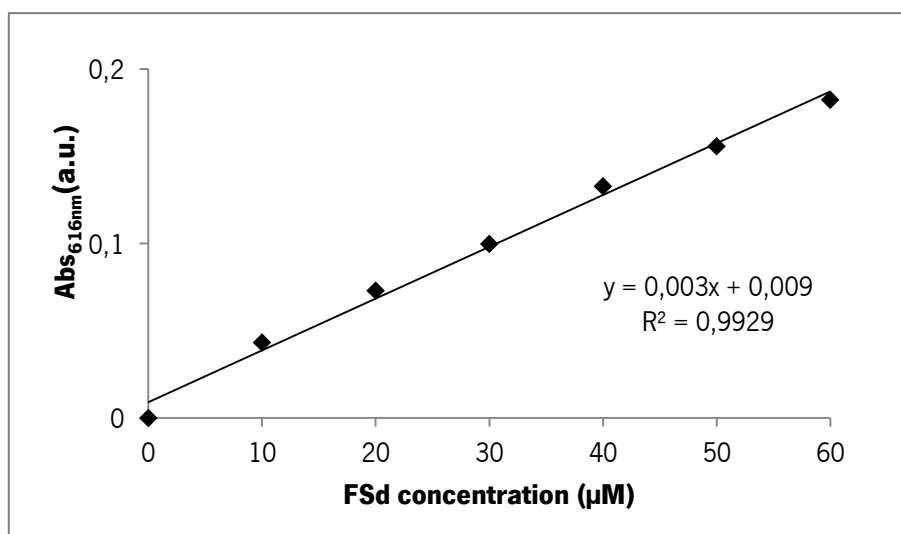


Figure B 2. Calibration curve of absorbance versus FSd dye concentration.

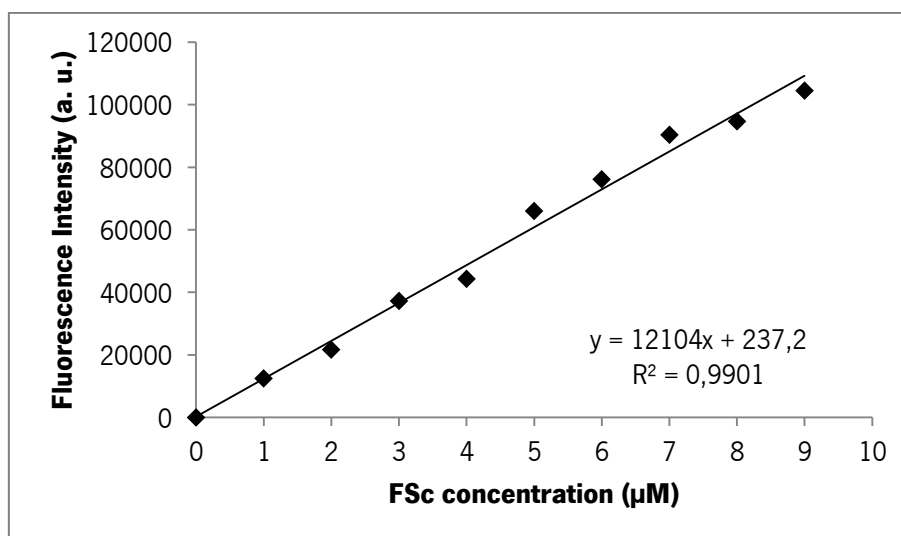


Figure B 3. Calibration curve of fluorescence intensity versus FSc dye concentration.

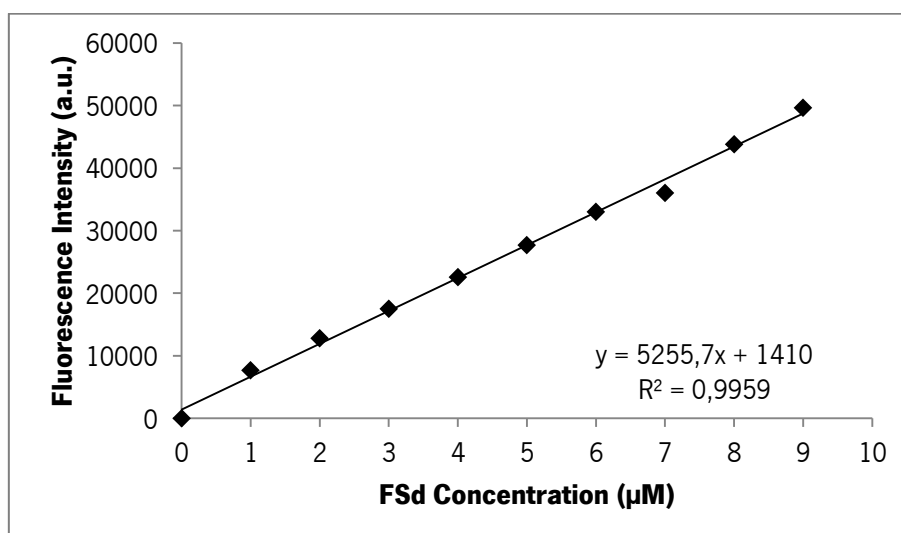


Figure B 4. Calibration curve of fluorescence intensity versus FSd dye concentration.